

# On Constrained Langevin Equations and (Bio)Chemical Reaction Networks

David F. Anderson<sup>1</sup>, Desmond J. Higham<sup>2</sup>, Saul C. Leite<sup>3</sup>, and Ruth J. Williams<sup>4</sup>

## Abstract

Stochastic effects play an important role in modeling the time evolution of chemical reaction systems in fields such as systems biology, where the concentrations of some constituent molecules can be low. The most common stochastic models for these systems are continuous time Markov chains, which track the molecular abundance of each chemical species. Often, these stochastic models are studied by computer simulations, which can quickly become computationally expensive. A common approach to reduce computational effort is to approximate the discrete valued Markov chain by a continuous valued diffusion process. However, existing diffusion approximations either do not respect the constraint that chemical concentrations are never negative (linear noise approximation) or are typically only valid until the concentration of some chemical species first becomes zero (chemical Langevin equation).

In this paper, we propose (obliquely) reflected diffusions, which respect the non-negativity of chemical concentrations, as approximations for Markov chain models of chemical reaction networks. These reflected diffusions satisfy “constrained Langevin equations,” in that they behave like solutions of chemical Langevin equations in the interior of the positive orthant and are constrained to the orthant by instantaneous oblique reflection at the boundary. To motivate their form, we first illustrate our constrained Langevin approximations for two simple examples. We then describe the general form of our proposed approximation. We illustrate the performance of our approximations through comparison of their stationary distributions for the two examples with those of the Markov chain model and through simulations of more complex examples.

**MSC 2010 subject classifications:** Primary 60J28, 60J60, 65C30, 92C45; Secondary 60H10, 65C40, 92C40.

**Keywords:** Density dependent Markov chains, diffusion approximation, Langevin equation, linear noise approximation, chemical reaction networks, stochastic differential equation with reflection, systems biology.

## 1 Introduction

Reacting chemical species are often modeled by deterministic differential equations representing the time evolution of molecular concentrations. Nonetheless, at a finer scale, chemical reaction systems are fundamentally stochastic in nature. Deterministic models provide a mean field approximation to these systems and are generally good predictors when the abundances of all species are high enough to average out the stochastic fluctuations. However, in some applications, such as in systems biology, not every molecular species is present in large numbers. The most common stochastic model of chemical kinetics treats the system as a continuous time Markov chain that tracks the (integer-valued) number of molecules of each chemical species [2, 17, 43]. These Markov chain models are often studied by sample path simulation in order to get Monte Carlo estimates for desired quantities [14, 15, 16]. However, these simulations can quickly

---

<sup>1</sup>Department of Mathematics, University of Wisconsin - Madison, Madison, WI, 53706, USA, anderson@math.wisc.edu

<sup>2</sup>Department of Mathematics and Statistics, University of Strathclyde, Glasgow, G1 1XH, UK, d.j.higham@strath.ac.uk

<sup>3</sup>Centro de Matemática, Computação e Cognição, UFABC, Santo André, SP 09210-580, Brazil, saul.leite@ufabc.edu.br

<sup>4</sup>Department of Mathematics, University of California - San Diego, La Jolla, CA, 92093-0112 USA, williams@math.ucsd.edu

become computationally expensive when some reactions are very fast, since every reaction is individually accounted for. When the abundances of the chemical species are large (but not large enough to ignore the influence of stochastic fluctuations) the units can be converted from abundances to concentrations and the solutions to the continuous time Markov chain model can be approximated by solutions to Stochastic Differential Equations (SDEs). The resulting solutions are usually called a diffusion approximation; see, for example, [25]. These diffusion approximations can be simulated by numerical methods for SDEs, where a fixed time step can be set, yielding more efficient simulations in most cases. While the standard continuous time Markov chain model satisfies the natural condition that all abundances remain non-negative for all time, diffusion approximations do not, in general, respect such a non-negativity condition.

There are two commonly used diffusion approximations for the Markov chain model, the linear noise approximation [39, 40] and the chemical Langevin equation [18, 19, 25]. The linear noise approximation is obtained by linearizing fluctuations about the deterministic approximation. Although this approximation is well defined for all times, it typically diffuses outside of the positive orthant, predicting negative concentration values. In addition, it is well known [34, 41] that it can fail to capture fluctuations due to nonlinearities in the reaction rate functions. On the other hand, the chemical Langevin equation is known to give better approximations than the linear noise approximation when nonlinearities are present. However, the chemical Langevin equation is usually not defined beyond the first time the boundary of the orthant is reached. In fact, since the diffusion terms of the equation typically involve square roots of the molecular concentration, the unstopped equation becomes ill posed [28, 36, 42].

For example, consider the following simple reaction system in which a molecule of  $S_1$  can be converted to a molecule of  $S_2$  and vice versa:



where  $\beta_1, \beta_2 > 0$  are the rate constants and we assume the corresponding propensities follow mass action kinetics. When the number of  $S_1$  molecules reaches zero in the Markov chain model, the reaction  $S_1 \rightarrow S_2$  has zero intensity and cannot proceed until another  $S_1$  molecule is created via the reaction  $S_2 \rightarrow S_1$ . In this manner non-negativity of the number of  $S_1$  molecules is preserved. Of course, a symmetric argument shows that the number of  $S_2$  molecules remains non-negative for all time. However, denoting the concentration of  $S_i$  at time  $t$  by  $x_i(t)$ , the usual chemical Langevin equation for this model consists of the system of SDEs:

$$dx_1(t) = (-\beta_1 x_1(t) + \beta_2 x_2(t))dt - \frac{1}{\sqrt{r}} \sqrt{\beta_1 x_1(t)} dW_1(t) + \frac{1}{\sqrt{r}} \sqrt{\beta_2 x_2(t)} dW_2(t) \quad (2)$$

$$dx_2(t) = (\beta_1 x_1(t) - \beta_2 x_2(t))dt + \frac{1}{\sqrt{r}} \sqrt{\beta_1 x_1(t)} dW_1(t) - \frac{1}{\sqrt{r}} \sqrt{\beta_2 x_2(t)} dW_2(t), \quad (3)$$

where  $W_1$  and  $W_2$  are independent Brownian motions, the equations are interpreted in the Itô sense, and  $r$  is usually taken to be Avogadro's number multiplied by the volume of the vessel in which the reactions are taking place. Whenever  $x_1(t)$  is near zero

$$\beta_2 x_2(t)dt + \frac{1}{\sqrt{r}} \sqrt{\beta_2 x_2(t)} dW_2(t) \quad (4)$$

is the dominant term in the right hand side of equation (2). Because the term involving  $W_2$  in (4) is as likely to push  $x_1$  in the negative direction as in the positive direction,  $x_1$  can become negative, thereby making equation (2) nonsensical in our context. Of course, a symmetric argument shows that  $x_2(t)$  can become negative due to the stochastic forcing from  $W_1$ .

In this paper, we propose a *constrained Langevin approximation* for chemical reaction systems which is a reflected diffusion satisfying a non-negativity constraint. In order to motivate the approximation, we begin with two simple, but natural, one-dimensional examples and then extend the approximation to the general

multidimensional case. For the one-dimensional models, we also show how to compute stationary distributions for the approximation. It is worth noting that because the constrained Langevin approximation is developed via the same first principle arguments used in the development of the standard chemical Langevin equation, solutions to the two models satisfy the same dynamics within the strictly positive orthant. This fact is in contrast to other Langevin type models developed to fix the negativity problem that perturb the dynamics globally to fix what is inherently a local (to the boundary) problem [42]. We emphasize that the derivation in this paper of the constrained Langevin approximation is only formal. The paper [27] is a rigorous technical complement to this paper. In [27], under mild conditions, the well posedness of the reflected diffusion is proved and it is shown that this diffusion process can be achieved as a weak limit of a sequence of jump-diffusion Markov processes that mimic the Langevin system in the interior of the positive orthant and behave like a scaled version of the Markov chain on the boundary.

In related work, several authors have devised approaches that combine the accuracy and robustness of the Markov chain model with the computational efficiency of the Langevin diffusion or ODE models; see, for example, [4, 10, 13, 20] and the references therein. For example, hybrid models have been proposed that exploit the existence of fast and slow reactions (determined either a priori or dynamically) [13, 20] or blend the jump and diffusion models, depending on the current system state [4, 10]. In a different vein, in [33] it has been proposed to extend the range of solutions for the Langevin equation to the complex numbers. The authors of [33] illustrate their approximation for some unimolecular and bimolecular examples. Although this state representation loses physical meaning, the authors show that this “complex Langevin equation” can be used to give real-valued approximations to moments and first passage times. Our work has a different focus to the references mentioned above. We operate entirely in the diffusion setting and introduce a general strategy to respect non-negativity and well posedness. This permits simulation of sample paths and avoids the need for ad hoc thresholding, blending parameters or introducing additional state variables and does not require specialized assumptions on the structure of the reaction system.

The rest of this paper is organized as follows. Section 1.1 gives a short description of the notation which will be used throughout the paper. In Section 2, we present the continuous time Markov chain model for chemical reaction networks, beginning with its most common form in Section 2.1, where the state represents the number of molecules of each species in the system. Next, in Section 2.2, we introduce the scaled Markov chain model, where the state representation is converted from abundances to molecular concentrations. The constrained Langevin approximation is presented in Section 3. We begin by introducing two motivating one-dimensional examples in Section 3.1 and the ideas are then extended to the general multidimensional case in Section 3.2. Section 4 is dedicated to numerical results, where we compare the constrained Langevin approximation with the Markov chain model and the linear noise approximation. We begin by comparing the stationary distributions of the one-dimensional examples in Section 4.1 and, later, in Section 4.2, we present the result of computer simulations for two-dimensional examples.

## 1.1 Notation

For any integer  $m \geq 1$ , let  $\mathbb{Z}^m$  denote the integer lattice and  $\mathbb{Z}_{\geq 0}^m$  denote the integer lattice of points with non-negative components. Let  $\mathbb{R}^m$  denote the  $m$ -dimensional Euclidean space and let  $\mathbb{R}_{\geq 0}^m$  denote the positive orthant in  $\mathbb{R}^m$  (i.e., the set of points of  $\mathbb{R}^m$  whose components are all non-negative). When  $m = 1$ , we write  $\mathbb{Z}^1$ ,  $\mathbb{Z}_{\geq 0}^1$ ,  $\mathbb{R}^1$ , and  $\mathbb{R}_{\geq 0}^1$  as  $\mathbb{Z}$ ,  $\mathbb{Z}_{\geq 0}$ ,  $\mathbb{R}$  and  $\mathbb{R}_{\geq 0}$ , respectively. For a vector  $x \in \mathbb{R}^m$ , we denote by  $x'$  its transpose and for a given set of vectors  $\{x_1, \dots, x_d\} \subset \mathbb{R}^m$ , we denote by  $\text{span}\{x_1, \dots, x_d\}$  the set of all linear combinations of its elements. For sets  $A$  and  $B$  such that  $A \subset B$ , we denote by  $1_A : B \rightarrow \mathbb{R}$  the indicator function, where  $1_A(x)$  is defined to be 1 when  $x \in A$  and 0 otherwise, for all  $x \in B$ .

## 2 Markov chain model of chemical reaction systems

We consider a chemical reaction system consisting of a finite set of species  $\{S_1, S_2, \dots, S_m\}$  involved in  $K$  possible reactions, where  $K$  is a positive integer. For  $k \in \{1, \dots, K\}$ , we denote by  $v_k^-$  and  $v_k^+$  the vectors in  $\mathbb{Z}_{\geq 0}^m$  such that  $v_{ik}^-$  and  $v_{ik}^+$  (the  $i$ th component of each) give the numbers of molecules of the  $i$ th species consumed and produced in the  $k$ th reaction, respectively. For example, if the  $k$ th reaction in a system consisting of just two species is  $2S_1 \rightarrow S_2$ , then  $v_k^- = \begin{bmatrix} 2 \\ 0 \end{bmatrix}$  and  $v_k^+ = \begin{bmatrix} 0 \\ 1 \end{bmatrix}$ . We denote by  $X(t)$  the vector in  $\mathbb{Z}_{\geq 0}^m$  whose  $i$ th component gives the number of molecules of the  $i$ th species at time  $t$ . We note that occurrence of the  $k$ th reaction at a time  $t$  changes the state of the system by addition of the reaction vector  $v_k = v_k^+ - v_k^-$ ; that is,

$$X(t) = X(t-) + v_k.$$

We assume that  $v_k \neq 0$  for each  $k = 1, \dots, K$ . In the next subsection, we describe the usual continuous time Markov chain model for such systems.

### 2.1 Continuous time Markov chain model

The standard stochastic model for a chemical system treats the system as a continuous time, discrete state Markov chain [17, 43]. To each reaction there is an associated real valued function of the state,  $\Lambda_k : \mathbb{Z}_{\geq 0}^m \rightarrow \mathbb{R}_{\geq 0}$ , called the *propensity* or *intensity* function, giving the rate at which the  $k$ th reaction occurs. Specifically, it is assumed that for each  $k \in \{1, \dots, K\}$ ,  $x \in \mathbb{Z}_{\geq 0}^m$  and  $t \geq 0$ ,

$$\begin{aligned} P\{X(t + \Delta t) = x + v_k \mid X(t) = x\} &= \Lambda_k(x)\Delta t + o(\Delta t) \\ P\{X(t + \Delta t) = x \mid X(t) = x\} &= \left(1 - \sum_{k=1}^K \Lambda_k(x)\Delta t\right) + o(\Delta t) \end{aligned} \quad (5)$$

where  $o(\Delta t)/\Delta t \rightarrow 0$ , as  $\Delta t \rightarrow 0$ . The usual assumption on the intensity functions  $\Lambda_k$ , and the assumption we make throughout, is that they satisfy *stochastic mass action kinetics*: for  $x \in \mathbb{Z}_{\geq 0}^m$  the rate of the  $k$ th reaction is

$$\Lambda_k(x) = \kappa_k \prod_{i=1}^m (x_i)_{v_{ik}^-}, \quad (6)$$

for some constant  $\kappa_k > 0$ , where

$$(x_i)_{v_{ik}^-} = x_i(x_i - 1) \dots (x_i - v_{ik}^- + 1) = \frac{x_i!}{(x_i - v_{ik}^-)!}. \quad (7)$$

The constant  $\kappa_k$  is called the (*stochastic*) *reaction rate constant*.

For example, zeroth order reactions of the form  $\emptyset \rightarrow S_1$  have constant rate function  $\Lambda_k(x) = \kappa_k$ , first order reactions of the forms  $S_1 \rightarrow S_2$  or  $S_1 \rightarrow \emptyset$  have rate  $\Lambda_k(x) = \kappa_k x_1$ , and second order reactions of the forms  $S_1 + S_2 \rightarrow S_3$  and  $2S_1 \rightarrow S_3$  have respective rates  $\Lambda_k(x) = \kappa_k x_1 x_2$  and  $\Lambda_k(x) = \kappa_k x_1(x_1 - 1)$ . Thus, the rate (6) is proportional to the number of distinct subsets of the molecules present that can form the inputs for the reaction. Intuitively, the mass action assumption reflects the idea that the system is *well-stirred* in the sense that all molecules are equally likely to be at any location at any time.

There are different ways to represent the Markov chain model having the properties described in (5), however we find the following endogenous representation for the Markov chain to be very useful. In this representation, the Markov chain  $X(t)$  is given as the solution of the following equation:

$$X(t) = X(0) + \sum_{k=1}^K v_k N_k \left( \int_0^t \Lambda_k(X(s)) ds \right), \quad (8)$$

where  $N_k$ , for  $k \in \{1, \dots, K\}$ , are independent unit-rate Poisson processes<sup>1</sup>, and, for each  $k$ , the time changed Poisson process  $N_k(\int_0^t \Lambda_k(X(s))ds)$  represents the number of times the  $k$ th reaction has occurred by time  $t$  (for more on this representation see, for example, [2], Chapter 6 of [12], or [26]).

## 2.2 Scaled System

We may convert from abundances to concentrations. To indicate the dependence of quantities such as  $X$  on the volume of the vessel in which the reactions are occurring, we let  $r$  denote the volume of the vessel multiplied by Avogadro's number and we append a superscript  $r$  to  $X$  (and other quantities that depend on  $r$ ). Define  $\bar{X}_i^r(\cdot) = \frac{1}{r} X_i^r(\cdot)$ , for  $i = 1, \dots, m$ . Note that  $\bar{X}_i^r(t)$  is simply the concentration of the  $i$ th species in moles per unit volume at time  $t \geq 0$ . As the units of the stochastic rate law are in *numbers* of molecules, but the units of  $\bar{X}^r$  are moles per unit volume, to be able to write a sensible equation governing the dynamics of  $\bar{X}^r$ , the rates must also be scaled by  $r$  in an appropriate manner. The standard scaling (see for example Chapter 6 of [43]) is the following: for zeroth order reactions, the stochastic rate constant  $\kappa_k^r$  is equal to  $rc_k$  for some  $c_k > 0$  that does not depend upon  $r$ ; for first order reactions,  $\kappa_k^r = c_k$ ; and for second order reactions,  $\kappa_k^r = c_k/r$ . In general, for  $j$ th order reactions,  $\kappa_k^r = c_k r^{-j+1}$ .

Let  $\Lambda_k^r$  denote the propensity function for the  $k$ th reaction that is associated with the system indexed by  $r$ , when following stochastic mass action kinetics as in (6), with rate constant  $\kappa_k^r$  satisfying the scaling detailed in the previous paragraph. Define

$$\lambda_k(x) = c_k \prod_{i=1}^m x_i^{v_{ik}^-},$$

for  $x \in \mathbb{R}_{\geq 0}^m$ , where we take  $0^0 \equiv 1$ . This  $\lambda_k$  is the reaction rate function associated with *deterministic mass action kinetics*, with reaction rate constant  $c_k$ . It is an exercise to check that for any reaction, i.e., zeroth order, first order, second order, etc.,

$$\Lambda_k^r(X^r(t)) = r\lambda_k(\bar{X}^r(t)) + \epsilon_k^r(\bar{X}^r(t)),$$

where  $\epsilon_k^r(x)$  is a multivariate polynomial in the coordinates of  $x$  and  $1/r$  that is uniformly bounded for all  $r \geq 1$  as  $x$  varies in a compact set, and is non-zero only if the  $k$ th reaction consumes more than one molecule of a particular species. For example, for the second order reaction  $S_1 + S_2 \rightarrow S_3$  we have

$$\Lambda_k^r(X^r(t)) = \frac{c_k}{r} (r\bar{X}_1^r(t)) (r\bar{X}_2^r(t)) = rc_k \bar{X}_1^r(t) \bar{X}_2^r(t) = r\lambda_k(\bar{X}^r(t)),$$

whereas for the second order reaction  $2S_1 \rightarrow S_3$  we have

$$\Lambda_k^r(X^r(t)) = \frac{c_k}{r} r\bar{X}_1^r(t) (r\bar{X}_1^r(t) - 1) = rc_k \bar{X}_1^r(t)^2 - c_k \bar{X}_1^r(t) = r\lambda_k(\bar{X}^r(t)) + \epsilon_k^r(\bar{X}^r(t)),$$

with  $\epsilon_k^r(x) = -c_k x_1$ .

After performing the above scaling from *numbers* of molecules to *concentrations*, and defining

$$\lambda_k(x) = \frac{\Lambda_k^r(rx)}{r} = \lambda_k(x) + (1/r)\epsilon_k^r(x), \quad (9)$$

equation (8) yields

$$\bar{X}^r(t) = \bar{X}^r(0) + \frac{1}{r} \sum_{k=1}^K v_k N_k \left( r \int_0^t \lambda_k(\bar{X}^r(s)) ds \right). \quad (10)$$

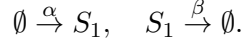
<sup>1</sup>Recall,  $N_k$  is a unit-rate Poisson process if  $N_k(0) = 0$ ,  $N_k(\cdot)$  has independent increments, and  $N_k(t+s) - N_k(s)$  has a Poisson distribution with parameter  $t$  for all  $t, s \geq 0$ .

### 3 The constrained Langevin approximation

We start by presenting two examples that serve to motivate our constrained Langevin approximation for the model (10). We stress that, as there are no limit theorems given here, the arguments are meant to show the plausibility of the proposed approximation.

#### 3.1 Motivating examples

**Example 1.** Consider the chemical reaction system with the two reactions



The constants  $\alpha > 0$  and  $\beta > 0$  over the arrows here denote the (deterministic) reaction rate constants  $c_1$  and  $c_2$  for the two reactions. Then, with the scaling of propensities described in Section 2.2, the Markov chain  $X^r(\cdot)$ , which models the stochastic dynamics of the number of molecules of  $S_1$  when the volume measure is  $r$ , satisfies

$$X^r(t) = X^r(0) + N_1(r\alpha t) - N_2\left(\int_0^t \beta X^r(s) ds\right), \quad (11)$$

where  $N_1$  and  $N_2$  are independent, unit-rate Poisson processes.

Let  $G = [0, \infty)$ ,  $G^\circ = (0, \infty)$ , the interior of  $G$ , and  $G^b = \{0\}$ , the boundary of  $G$ . We now give an equivalent in distribution representation of  $X^r$ , where we separately consider jumps of  $X^r$  from the interior of  $G$  and from the boundary of  $G$ . Specifically, an equivalent in distribution representation for  $X^r$  is:

$$\begin{aligned} X^r(t) = X^r(0) &+ N_1^o\left(r\alpha \int_0^t 1_{\{X^r(s) \in G^\circ\}} ds\right) + N_1^b\left(r\alpha \int_0^t 1_{\{X^r(s) \in G^b\}} ds\right) \\ &- N_2^o\left(\int_0^t \beta X^r(s) 1_{\{X^r(s) \in G^\circ\}} ds\right) - N_2^b\left(\int_0^t \beta X^r(s) 1_{\{X^r(s) \in G^b\}} ds\right), \end{aligned} \quad (12)$$

where  $N_1^o, N_1^b, N_2^o, N_2^b$  are independent unit-rate Poisson processes. (The distributional equivalence of the two solution processes in (11) and (12) can be understood informally via the superposition property of Poisson processes. See Chapter 1 of [3] for a rigorous argument.)

Recall the definition from Section 2.2 of  $\bar{X}^r(\cdot) = \frac{1}{r}X^r(\cdot)$ , the normalized (concentration-valued) process. For this example, the process satisfies

$$\begin{aligned} \bar{X}^r(t) = \bar{X}^r(0) &+ \frac{1}{r}N_1^o\left(r\alpha \int_0^t 1_{\{\bar{X}^r(s) \in G^\circ\}} ds\right) + \frac{1}{r}N_1^b\left(r\alpha \int_0^t 1_{\{\bar{X}^r(s) \in G^b\}} ds\right) \\ &- \frac{1}{r}N_2^o\left(r \int_0^t \beta \bar{X}^r(s) 1_{\{\bar{X}^r(s) \in G^\circ\}} ds\right) - \frac{1}{r}N_2^b\left(r \int_0^t \beta \bar{X}^r(s) 1_{\{\bar{X}^r(s) \in G^b\}} ds\right). \end{aligned} \quad (13)$$

We can center a unit-rate Poisson process  $N$  about its mean by defining  $\hat{N}(t) = N(t) - t$ , for all  $t \geq 0$ . Centering  $N_1^o$  and  $N_2^o$  in this way, collecting terms in an obvious manner, and noting that the last term in (13) is identically equal to zero (since  $x1_{\{x=0\}} \equiv 0$ ), we see that  $\bar{X}^r$  satisfies

$$\begin{aligned} \bar{X}^r(t) = \bar{X}^r(0) &+ \alpha \int_0^t 1_{\{\bar{X}^r(s) \in G^\circ\}} ds - \int_0^t \beta \bar{X}^r(s) 1_{\{\bar{X}^r(s) \in G^\circ\}} ds \\ &+ \frac{1}{\sqrt{r}} \left[ \frac{1}{\sqrt{r}} \hat{N}_1^o\left(r\alpha \int_0^t 1_{\{\bar{X}^r(s) \in G^\circ\}} ds\right) - \frac{1}{\sqrt{r}} \hat{N}_2^o\left(r \int_0^t \beta \bar{X}^r(s) 1_{\{\bar{X}^r(s) \in G^\circ\}} ds\right) + \check{Y}^r(t) \right], \end{aligned} \quad (14)$$



where  $\check{Y}^r(t) = \frac{1}{\sqrt{r}}N_1^b\left(r\alpha\int_0^t 1_{\{\bar{X}^r(s)\in G^b\}}ds\right)$ ,  $t \geq 0$ , defines a non-decreasing jump process, which can only jump at times  $s$  for which  $\bar{X}^r(s-)$  is at the boundary of  $G$ .

Our goal is to propose a diffusion process defined on  $[0, \infty)$  that approximates  $\bar{X}^r$  for fixed  $r$  of moderate size. By the functional central limit theorem for a centered, unit-rate Poisson process  $\hat{N}$ , we have that  $\frac{1}{\sqrt{r}}\hat{N}(r\cdot)$  is well approximated in distribution by  $\widehat{W}(\cdot)$ , a standard one-dimensional Brownian motion<sup>2</sup>. This suggests that for an approximation, we replace  $\frac{1}{\sqrt{r}}\hat{N}_k^\circ(r\cdot)$  by  $\widehat{W}_k^\circ(\cdot)$ , for  $k = 1, 2$ , in (14), where  $\widehat{W}_1^\circ$  and  $\widehat{W}_2^\circ$  are independent standard one-dimensional Brownian motions. Inserting these approximations in equation (14) and replacing  $\bar{X}^r, \check{Y}^r$  with  $Z^r, Y^r$ , respectively, leads us to propose approximating  $\bar{X}^r$  by a jump-diffusion process  $Z^r$  satisfying

$$\begin{aligned} Z^r(t) = & Z^r(0) + \int_0^t (\alpha - \beta Z^r(s)) 1_{\{Z^r(s) \in G^\circ\}} ds + \frac{1}{\sqrt{r}} \widehat{W}_1^\circ \left( \alpha \int_0^t 1_{\{Z^r(s) \in G^\circ\}} ds \right) \\ & - \frac{1}{\sqrt{r}} \widehat{W}_2^\circ \left( \int_0^t \beta Z^r(s) 1_{\{Z^r(s) \in G^\circ\}} ds \right) + \frac{1}{\sqrt{r}} Y^r(t), \end{aligned} \quad (15)$$

where  $Y^r(t) = \frac{1}{\sqrt{r}}N_1^b\left(r\alpha\int_0^t 1_{\{Z^r(s)\in G^b\}}ds\right)$ . By a martingale representation theorem (see e.g., Theorem 4.2 of [23], page 170), the difference of the two processes  $\widehat{W}_1^\circ\left(\alpha\int_0^t 1_{\{Z^r(s)\in G^\circ\}}ds\right)$  and  $\widehat{W}_2^\circ\left(\int_0^t \beta Z^r(s) 1_{\{Z^r(s)\in G^\circ\}}ds\right)$  (which are local martingales) can be represented as the single stochastic integral process

$$\int_0^t \sqrt{\alpha + \beta Z^r(s)} 1_{\{Z^r(s) \in G^\circ\}} dW(s), \quad (16)$$

where  $W$  is a standard one-dimensional Brownian motion.

Since we seek a diffusion approximation that moves continuously and spends zero time (in the sense of Lebesgue measure) at any particular point in  $[0, \infty)$ , it is reasonable to suppress the indicator functions in (15) and to replace the jump process  $Y^r$  by a continuous non-decreasing process that increases only when our diffusion process is on the boundary. This leads to a proposed reflected diffusion approximation  $\tilde{Z}^r$  for  $\bar{X}^r$  that satisfies

$$\tilde{Z}^r(t) = \tilde{Z}^r(0) + \int_0^t (\alpha - \beta \tilde{Z}^r(s)) ds + \frac{1}{\sqrt{r}} \int_0^t \sqrt{\alpha + \beta \tilde{Z}^r(s)} d\widetilde{W}(s) + \frac{1}{\sqrt{r}} \tilde{Y}^r(t), \quad (17)$$

where  $\widetilde{W}$  is a standard one-dimensional Brownian motion, and where  $\tilde{Y}^r$  is a continuous, non-decreasing process that only increases when  $\tilde{Z}^r$  is zero. The process  $\frac{1}{\sqrt{r}}\tilde{Y}^r$  tracks the cumulative amount of pushing at the boundary required to keep  $\tilde{Z}^r$  non-negative and is usually referred to as the *reflection* or *local time* term. Although the  $\frac{1}{\sqrt{r}}$  scale factor could be absorbed into  $\tilde{Y}^r$ , we keep it separate here to indicate that this reflection term is expected to be of the same order as the noise term, i.e., of order  $\frac{1}{\sqrt{r}}$ , to counter the excursions of the stochastic integral term involving  $\widetilde{W}$  that try to drive  $\tilde{Z}^r$  negative. It is known<sup>3</sup> that given a pair  $(\tilde{Z}^r(0), \widetilde{W})$ , there exists a unique solution  $\tilde{Z}^r$  to (17) that lives in  $[0, \infty)$  and is adapted to  $\tilde{Z}^r(0)$  and  $\widetilde{W}$ . The process  $\tilde{Z}^r$  is a diffusion on  $[0, \infty)$  with state dependent drift coefficient  $x \mapsto \alpha - \beta x$ , dispersion coefficient  $x \mapsto \frac{1}{\sqrt{r}}\sqrt{\alpha + \beta x}$ , and instantaneous reflection at the origin.

<sup>2</sup>Indeed, one can even do this in a strong way. One can construct  $N(\cdot)$  and  $\widehat{W}(\cdot)$  on the same probability space so that  $N(t) = t + \widehat{W}(t) + \xi(t)$  for all  $t \geq 0$ , where  $\sup_{t \geq 0} \frac{\xi(t)}{\log(2\sqrt{t})}$  is a random variable with a finite exponential moment (see Corollary 5.5 of [12, pg. 359] and [24]).

<sup>3</sup>This follows from the uniform Lipschitz property of the drift and dispersion coefficient, and the Lipschitz continuity of the so-called Skorokhod map that defines the reflection at the origin (i.e., determines  $\tilde{Y}^r$ ) in terms of the other parts of the equation. In this case with normal reflection at the boundary, a rigorous justification follows from the work of Tanaka [37].

Notice that ignoring terms in (17) of order  $\frac{1}{\sqrt{r}}$  leads to the usual deterministic approximation to the scaled model (13). The term  $\frac{1}{\sqrt{r}} \int_0^t \sqrt{\alpha + \beta \tilde{Z}^r(s)} d\tilde{W}(s)$  captures stochastic fluctuations. The term  $\frac{1}{\sqrt{r}} \tilde{Y}^r$  only comes into play when  $\tilde{Z}^r$  is zero, and provides a minimal restoring force to keep  $\tilde{Z}^r$  non-negative.

**Example 2.** Consider the chemical reaction system given in (1). For  $i \in \{1, 2\}$ , let  $X_i^r(t)$  denote the number of molecules of  $S_i$  at time  $t$ . Let  $M^r = X_1^r(0) + X_2^r(0)$ , which is a conserved quantity. The process  $X_1^r$  can be represented as a solution to

$$X_1^r(t) = X_1^r(0) - N_1 \left( \int_0^t \beta_1 X_1^r(s) ds \right) + N_2 \left( \int_0^t \beta_2 (M^r - X_1^r(s)) ds \right), \quad (18)$$

where  $N_1$  and  $N_2$  are independent, unit-rate Poisson processes, and  $X_2^r(\cdot) \equiv M^r - X_1^r(\cdot)$ .

In a similar manner to that used in Example 1, let  $G^r = [0, M^r]$ ,  $G^{\circ,r} = (0, M^r)$ , the interior of  $G^r$ , and  $G^{b,r} = \{0, M^r\}$ , the boundary of  $G^r$ . A distributionally equivalent way to represent  $X_1^r$  is as a solution of

$$\begin{aligned} X_1^r(t) = & X_1^r(0) - N_1^o \left( \int_0^t \beta_1 X_1^r(s) 1_{\{X_1^r(s) \in G^{\circ,r}\}} ds \right) - N_1^b \left( \int_0^t \beta_1 X_1^r(s) 1_{\{X_1^r(s) \in G^{b,r}\}} ds \right) \\ & + N_2^o \left( \int_0^t \beta_2 (M^r - X_1^r(s)) 1_{\{X_1^r(s) \in G^{\circ,r}\}} ds \right) + N_2^b \left( \int_0^t \beta_2 (M^r - X_1^r(s)) 1_{\{X_1^r(s) \in G^{b,r}\}} ds \right), \end{aligned} \quad (19)$$

where  $N_1^o, N_1^b, N_2^o, N_2^b$  are independent unit-rate Poisson processes.

Now for the normalized process  $\bar{X}_1^r(\cdot) = \frac{1}{r} X_1^r(\cdot)$ , with  $\bar{M}^r = \frac{1}{r} M^r$ , the conserved quantity for the normalized process, we have that  $\bar{X}_1^r$  satisfies

$$\begin{aligned} \bar{X}_1^r(t) = & \bar{X}_1^r(0) - \frac{1}{r} N_1^o \left( r \int_0^t \beta_1 \bar{X}_1^r(s) 1_{\{\bar{X}_1^r(s) \in \hat{G}^{\circ,r}\}} ds \right) - \frac{1}{r} N_1^b \left( r \int_0^t \beta_1 \bar{X}_1^r(s) 1_{\{\bar{X}_1^r(s) \in \hat{G}^{b,r}\}} ds \right) \\ & + \frac{1}{r} N_2^o \left( r \int_0^t \beta_2 (\bar{M}^r - \bar{X}_1^r(s)) 1_{\{\bar{X}_1^r(s) \in \hat{G}^{\circ,r}\}} ds \right) \\ & + \frac{1}{r} N_2^b \left( r \int_0^t \beta_2 (\bar{M}^r - \bar{X}_1^r(s)) 1_{\{\bar{X}_1^r(s) \in \hat{G}^{b,r}\}} ds \right), \end{aligned} \quad (20)$$

where the normalized interior of the state space is  $\hat{G}^{\circ,r} = (0, \bar{M}^r)$  and the normalized boundary is  $\hat{G}^{b,r} = \{0, \bar{M}^r\}$ . Centering  $N_1^o$  and  $N_2^o$  and collecting terms, we see that  $\bar{X}_1^r$  satisfies

$$\begin{aligned} \bar{X}_1^r(t) = & \bar{X}_1^r(0) - \int_0^t \beta_1 \bar{X}_1^r(s) 1_{\{\bar{X}_1^r(s) \in \hat{G}^{\circ,r}\}} ds + \int_0^t \beta_2 (\bar{M}^r - \bar{X}_1^r(s)) 1_{\{\bar{X}_1^r(s) \in \hat{G}^{\circ,r}\}} ds \\ & + \frac{1}{\sqrt{r}} \left[ - \frac{1}{\sqrt{r}} \hat{N}_1^o \left( r \int_0^t \beta_1 \bar{X}_1^r(s) 1_{\{\bar{X}_1^r(s) \in \hat{G}^{\circ,r}\}} ds \right) \right. \\ & \left. + \frac{1}{\sqrt{r}} \hat{N}_2^o \left( r \int_0^t \beta_2 (\bar{M}^r - \bar{X}_1^r(s)) 1_{\{\bar{X}_1^r(s) \in \hat{G}^{\circ,r}\}} ds \right) - \check{Y}_1^r(t) + \check{Y}_2^r(t) \right], \end{aligned} \quad (21)$$

where  $\hat{N}_1^o$  and  $\hat{N}_2^o$  are centered versions of the Poisson processes  $N_1^o$  and  $N_2^o$ , respectively, and for  $t \geq 0$

$$\check{Y}_1^r(t) = \frac{1}{\sqrt{r}} N_1^b \left( r \int_0^t \beta_1 \bar{M}^r 1_{\{\bar{X}_1^r(s) = \bar{M}^r\}} ds \right), \quad \check{Y}_2^r(t) = \frac{1}{\sqrt{r}} N_2^b \left( r \int_0^t \beta_2 \bar{M}^r 1_{\{\bar{X}_1^r(s) = 0\}} ds \right),$$



are non-decreasing jump processes that only jump at times  $s$  for which  $\bar{X}^r(s-)$  equals  $\bar{M}^r$  or 0, respectively. These processes push  $\bar{X}_1^r$  back into  $\hat{G}^{\circ,r}$ . Note that some boundary jump terms in the expression for  $\bar{X}_1^r(t)$  have been eliminated here due to the facts that  $x1_{\{x=0\}} = 0$  and  $(\bar{M}^r - x)1_{\{x=\bar{M}^r\}} = 0$ .

Proceeding in a similar manner to that for Example 1, we approximate  $\frac{1}{\sqrt{r}}\hat{N}_k^o(r\cdot)$  by  $\widehat{W}_k^o(\cdot)$ , for  $k = 1, 2$ , where  $\widehat{W}_1^o$  and  $\widehat{W}_2^o$  are independent standard one-dimensional Brownian motions. This leads us to propose approximating  $\bar{X}_1^r$  by a jump-diffusion process  $Z_1^r$  that lives in  $[0, \bar{M}^r]$  and satisfies

$$\begin{aligned} Z_1^r(t) &= Z_1^r(0) + \int_0^t (-\beta_1 Z_1^r(s) + \beta_2(\bar{M}^r - Z_1^r(s))) 1_{\{Z_1^r(s) \in \hat{G}^{\circ,r}\}} ds \\ &\quad - \frac{1}{\sqrt{r}} W_1^o \left( \int_0^t \beta_1 Z_1^r(s) 1_{\{Z_1^r(s) \in \hat{G}^{\circ,r}\}} ds \right) + \frac{1}{\sqrt{r}} W_2^o \left( \int_0^t \beta_2(\bar{M}^r - Z_1^r(s)) 1_{\{Z_1^r(s) \in \hat{G}^{\circ,r}\}} ds \right) \\ &\quad - \frac{1}{\sqrt{r}} Y_1^r(t) + \frac{1}{\sqrt{r}} Y_2^r(t), \end{aligned} \quad (22)$$

$$Y_1^r(t) = \frac{1}{\sqrt{r}} N_1^b \left( r \int_0^t \beta_1 \bar{M}^r 1_{\{Z_1^r(s) = \bar{M}^r\}} ds \right), \quad Y_2^r(t) = \frac{1}{\sqrt{r}} N_2^b \left( r \int_0^t \beta_2 \bar{M}^r 1_{\{Z_1^r(s) = 0\}} ds \right).$$

Then using a martingale representation theorem, the difference of the two processes  $\widehat{W}_1^o \left( \int_0^t \beta_1 Z_1^r(s) 1_{\{Z_1^r(s) \in \hat{G}^{\circ,r}\}} ds \right)$  and  $\widehat{W}_2^o \left( \int_0^t \beta_2(\bar{M}^r - Z_1^r(s)) 1_{\{Z_1^r(s) \in \hat{G}^{\circ,r}\}} ds \right)$  (which are local martingales) can be represented as the single stochastic integral process

$$\int_0^t \sqrt{\beta_1 Z_1^r(s) + \beta_2(\bar{M}^r - Z_1^r(s))} 1_{\{Z_1^r(s) \in \hat{G}^{\circ,r}\}} dW(s), \quad (23)$$

where  $W$  is a standard one-dimensional Brownian motion.

As in Example 1, suppressing the indicator functions in (22) and replacing the jump processes  $Y_1^r, Y_2^r$  by continuous non-decreasing processes  $\tilde{Y}_1^r, \tilde{Y}_2^r$  that increase only when  $\tilde{Z}_1^r$  is at  $\bar{M}^r$  or 0, respectively, leads to a proposed reflected diffusion approximation  $\tilde{Z}_1^r$  for  $\bar{X}_1^r$  that satisfies

$$\begin{aligned} \tilde{Z}_1^r(t) &= \tilde{Z}_1^r(0) + \int_0^t (-\beta_1 \tilde{Z}_1^r(s) + \beta_2(\bar{M}^r - \tilde{Z}_1^r(s))) ds \\ &\quad + \frac{1}{\sqrt{r}} \int_0^t \sqrt{\beta_1 \tilde{Z}_1^r(s) + \beta_2(\bar{M}^r - \tilde{Z}_1^r(s))} d\tilde{W}(s) \\ &\quad - \frac{1}{\sqrt{r}} \tilde{Y}_1^r(t) + \frac{1}{\sqrt{r}} \tilde{Y}_2^r(t), \end{aligned} \quad (24)$$

where  $\tilde{W}$  is a standard, one-dimensional Brownian motion, and  $\tilde{Y}_1^r, \tilde{Y}_2^r$  are continuous, non-decreasing processes that only increase when  $\tilde{Z}_1^r$  is at  $\bar{M}^r$  or 0, respectively. It is known<sup>4</sup> that, given the pair  $(\tilde{Z}_1^r(0), \tilde{W})$ , there exists a solution to (24) that lives in  $[0, \bar{M}^r]$  and is adapted to  $\tilde{Z}_1^r(0)$  and  $\tilde{W}$ .

Notice again that ignoring terms in (24) of order  $\frac{1}{\sqrt{r}}$  leads to the usual deterministic approximation to the scaled model (19). The term  $\frac{1}{\sqrt{r}} \int_0^t \sqrt{\beta_1 \tilde{Z}_1^r(s) + \beta_2(\bar{M}^r - \tilde{Z}_1^r(s))} d\tilde{W}(s)$  captures stochastic fluctuations. The terms  $\frac{1}{\sqrt{r}} \tilde{Y}_1^r$  and  $\frac{1}{\sqrt{r}} \tilde{Y}_2^r$  only come into play when  $\tilde{Z}_1^r$  is on the boundary of the domain of interest and they provide a minimal restoring force to keep  $\tilde{Z}_1^r$  in that domain.

<sup>4</sup>Similarly to what was mentioned in respect to the solution of equation (17), this also follows from the work of Tanaka [37] by the uniform Lipschitz continuity of the drift, dispersion coefficient, and the Skorokhod map that defines the reflection, since the direction of reflection in this case is normal to the boundary.

In preparation for the general case, it is convenient to rewrite (24) as

$$\begin{aligned}\tilde{Z}_1^r(t) &= \tilde{Z}_1^r(0) + \int_0^t \mu^r(\tilde{Z}_1^r(s)) ds \\ &\quad + \frac{1}{\sqrt{r}} \int_0^t \sigma^r(\tilde{Z}_1^r(s)) d\tilde{W}(s) + \frac{1}{\sqrt{r}} \int_0^t n^r(\tilde{Z}_1^r(s)) d\tilde{L}^r(s),\end{aligned}$$

where  $\mu^r(x) = -\beta_1 x + \beta_2(\overline{M}^r - x)$ ,  $\sigma^r(x) = \sqrt{\beta_1 x + \beta_2(\overline{M}^r - x)}$ ,  $\tilde{L}^r(t) = \tilde{Y}_1^r(t) + \tilde{Y}_2^r(t)$  is continuous and non-decreasing and increases only when  $\tilde{Z}_1^r$  is on the boundary of  $\hat{G}^{\circ,r}$ , and  $n^r(x) = 1$  if  $x = 0$  and  $n^r(x) = -1$  if  $x = \overline{M}^r$  is the inward unit normal to the boundary of  $\hat{G}^{\circ,r}$ . The vector field  $n^r$  specifies the “direction” of reflection at the boundary. In this one-dimensional case, there is a unique (up to normalization) inward pointing direction (which is normal to the boundary). In the general case treated in the next subsection, more complicated boundary behavior occurs and the reflection direction is frequently not normal to the boundary.

### 3.2 The general case

We now consider the general case of a process  $\overline{X}^r$  satisfying (10). Let  $\mathcal{S} = \text{span}\{v_k, k = 1, \dots, K\}$  and let  $\hat{G}^r = (\overline{X}^r(0) + \mathcal{S}) \cap \mathbb{R}_{\geq 0}^m$ . Considering  $\hat{G}^r$  in  $\overline{X}^r(0) + \mathcal{S}$ , let  $\hat{G}^{\circ,r}$  and  $\hat{G}^{b,r}$  denote the relative interior and boundary of  $\hat{G}^r$ , respectively. Proceeding in a similar manner to that for the two examples given in the previous subsection, an equivalent in distribution representation for  $\overline{X}^r$  is given by

$$\begin{aligned}\overline{X}^r(t) &= \overline{X}^r(0) + \frac{1}{r} \sum_{k=1}^K v_k N_k^o \left( r \int_0^t \lambda_k^r(\overline{X}^r(s)) 1_{\{\overline{X}^r(s) \in \hat{G}^{\circ,r}\}} ds \right) \\ &\quad + \frac{1}{r} \sum_{k=1}^K v_k N_k^b \left( r \int_0^t \lambda_k^r(\overline{X}^r(s)) 1_{\{\overline{X}^r(s) \in \hat{G}^{b,r}\}} ds \right),\end{aligned}\tag{25}$$

where  $N_k^o, N_k^b$ ,  $k = 1, \dots, K$  are independent unit-rate Poisson processes. Upon centering the Poisson processes  $N_k^o$ ,  $k = 1, \dots, K$ , to obtain  $\hat{N}_k^o$ ,  $k = 1, \dots, K$ , we may rewrite the above as

$$\begin{aligned}\overline{X}^r(t) &= \overline{X}^r(0) + \sum_{k=1}^K v_k \int_0^t \lambda_k^r(\overline{X}^r(s)) 1_{\{\overline{X}^r(s) \in \hat{G}^{\circ,r}\}} ds \\ &\quad + \frac{1}{\sqrt{r}} \sum_{k=1}^K v_k \frac{1}{\sqrt{r}} \hat{N}_k^o \left( r \int_0^t \lambda_k^r(\overline{X}^r(s)) 1_{\{\overline{X}^r(s) \in \hat{G}^{\circ,r}\}} ds \right) \\ &\quad + \frac{1}{\sqrt{r}} \sum_{k=1}^K v_k \check{Y}_k^r(t),\end{aligned}\tag{26}$$

where  $\check{Y}_k^r(t) = \frac{1}{\sqrt{r}} N_k^b \left( r \int_0^t \lambda_k^r(\overline{X}^r(s)) 1_{\{\overline{X}^r(s) \in \hat{G}^{b,r}\}} ds \right)$ .

Noting the relation (9), it is natural to replace  $\lambda_k^r$  with  $\lambda_k$  to obtain approximate dynamics for  $\overline{X}^r$ . Also, as in the examples in the previous section, we can approximate  $\frac{1}{\sqrt{r}} \hat{N}_k^o(r \cdot)$  by  $\widehat{W}_k^o(\cdot)$ , for  $k = 1, \dots, K$ , where  $\widehat{W}_k^o$ ,  $k = 1, \dots, K$ , are independent standard one-dimensional Brownian motions. Let

$$\mu(x) = \sum_{k=1}^K v_k \lambda_k(x),\tag{27}$$

for each  $x \in \mathbb{R}_{\geq 0}^m$ . We suggest approximating  $\bar{X}^r$  by a jump-diffusion  $Z^r$  satisfying  $Z^r(0) = \bar{X}^r(0)$  and

$$\begin{aligned} Z^r(t) = & Z^r(0) + \int_0^t \mu(Z^r(s)) 1_{\{Z^r(s) \in \widehat{G}^{\circ, r}\}} ds \\ & + \frac{1}{\sqrt{r}} \sum_{k=1}^K v_k \widehat{W}_k^{\circ} \left( \int_0^t \lambda_k(Z^r(s)) 1_{\{Z^r(s) \in \widehat{G}^{\circ, r}\}} ds \right) \\ & + \frac{1}{\sqrt{r}} \sum_{k=1}^K v_k Y_k^r(t), \end{aligned} \quad (28)$$

where  $Y_k^r(t) = \frac{1}{\sqrt{r}} N_k^b \left( r \int_0^t \lambda_k(Z^r(s)) 1_{\{Z^r(s) \in \widehat{G}^{b, r}, Z^r(s) \geq v_k^-/r\}} ds \right)$ . Note that in the definition of  $Y_k^r$ , the indicator function suppresses jumps from the boundary that would require consumption of a given species when there is an insufficient amount of that species to make the transition possible. This is a small correction needed to account for the fact that the interior diffusion might occasionally bring  $Z^r$  to a point  $x$  on the boundary of  $\widehat{G}^r$  that cannot be reached by the discrete-valued process  $\bar{X}^r$  (which lives on a lattice), and where  $\lambda_k(x) > 0$ , and from which movement by  $Z^r$  along the vector  $-v_k^-$  would take  $Z^r$  outside of the positive orthant. Such occurrences are only possible when more than one component of  $Z^r$  is small, that is, whenever the process  $Z^r$  is near the intersection of two or more faces of the positive orthant. It is known that such occurrences are rare for some similar reflected diffusion processes<sup>5</sup>. Consequently, we anticipate this correction will likely be a relatively small one.

Using a martingale representation theorem (see e.g., Theorem 4.2 of [23], page 170), on a possibly enlarged probability space that accommodates a standard  $m$ -dimensional Brownian motion  $W$ , we can express  $\sum_{k=1}^K v_k \widehat{W}_k^{\circ} \left( \int_0^t \lambda_k(Z^r(s)) 1_{\{Z^r(s) \in \widehat{G}^{\circ, r}\}} ds \right)$  as the vector-valued stochastic integral process  $\int_0^t \sigma(Z^r(s)) 1_{\{Z^r(s) \in \widehat{G}^{\circ, r}\}} dW(s)$  where  $W$  is a standard  $m$ -dimensional Brownian motion,  $\sigma(x) = \sqrt{\Upsilon(x)}$  is the unique<sup>6</sup> positive semi-definite matrix-valued square root of the  $m \times m$  matrix

$$\Upsilon(x) = \sum_{k=1}^K v_k v_k' \lambda_k(x), \quad (29)$$

for  $x \in \mathbb{R}_{\geq 0}^m$ , and  $v_k'$  is the transpose of  $v_k$ .

**Remark.** The reader may note that the coefficients  $\mu$  and  $\sigma$  in the above do not depend on  $r$ . Example 1 in the previous subsection illustrates this, whereas our Example 2 has coefficients that appear to depend on  $r$ . However, the latter dependence occurs because, in that example, we have eliminated one of the variables, effectively projecting down to the concentration of  $S_1$  alone. Indeed, if we had written the approximation  $(\tilde{Z}_1^r, \tilde{Z}_2^r)$  for the concentrations of both species  $(\bar{X}_1^r, \bar{X}_2^r)$  satisfying  $\tilde{Z}_1^r + \tilde{Z}_2^r = \bar{M}^r$ , then in the notation of this subsection,  $\mu(x_1, x_2) = (-\beta_1 x_1 + \beta_2 x_2)v$  where  $v = (1, -1)'$ , and  $\sigma(x_1, x_2) = \sqrt{\frac{\beta_1 x_1 + \beta_2 x_2}{2}} v v'$ , which leads to an equivalent representation to that given for  $\tilde{Z}_1^r$  in (24).

To obtain an equation for our proposed diffusion approximation, we remove the indicator functions in the first two terms in (28), since the amount of time our diffusion approximation spends on the boundary is

<sup>5</sup>For some similar non-degenerate reflected diffusion processes (see Theorem 1 of [31] and Theorem 7.7 of [6]), it is known that the total amount of “pushing” done by the local-time term at the intersection of two or more boundary faces of the positive orthant is almost surely zero. Such local-time terms are approximate measures of the amount of time spent near boundary regions.

<sup>6</sup>The existence and uniqueness of a positive semi-definite square root for any positive semi-definite matrix is well known. Furthermore, the mapping from the matrix  $\Upsilon(x)$  to its square root  $\sigma(x)$  is Hölder continuous of order one-half. These results can be found in the book by Bhatia [7], for example.

zero (in the sense of Lebesgue measure). Furthermore, we want to replace the last term in (28), the boundary term, by a continuous process whose paths are locally of bounded variation and that only changes when the diffusion process is on the boundary  $\widehat{G}^{b,r}$ . In the examples in the previous section, the diffusion process was one-dimensional and there was a unique (up to normalization) direction at each boundary point in which the boundary process would push to keep the diffusion in the state space. In higher dimensions, there is much more freedom in the choice of such a direction. In the following we motivate our choice for this “reflection direction” in the general case.

In our reflected diffusion approximation, the role of the boundary term is to counteract fluctuations of the term driven by white noise that tends to take the diffusion process outside of the orthant. Since the fluctuations are of order  $\frac{1}{\sqrt{r}}$ , we expect this boundary term to be of order  $\frac{1}{\sqrt{r}}$ . This leads us to approximate  $N_k^b(\cdot)$  in  $Y_k^r$  by its deterministic rate process, and to ignore higher order terms, resulting in the following (formal) approximation:

$$\begin{aligned} \sum_{k=1}^K v_k Y_k^r(t) &\approx \sum_{k=1}^K \frac{v_k}{\sqrt{r}} \int_0^t r \lambda_k(Z^r(s)) 1_{\{Z^r(s) \in \widehat{G}^{b,r}, Z^r(s) \geq v_k^-/r\}} ds \\ &\approx \int_0^t \gamma(Z^r(s)) dL^r(s) \end{aligned} \quad (30)$$

where

$$\gamma(x) = \frac{\mu(x)}{|\mu(x)|} 1_{\{|\mu(x)| \neq 0\}} \text{ for } x \in \widehat{G}^{b,r}, \quad (31)$$

for  $\mu(x)$  given by (27), and where

$$L^r(t) = \sqrt{r} \int_0^t |\mu(Z^r(s))| 1_{\{Z^r(s) \in \widehat{G}^{b,r}\}} ds. \quad (32)$$

Note here that we have approximated the indicator function in (30) with the simpler indicator function in (32) (ignoring the rare effect mentioned after (28)).

The process  $L^r$  is a weighted and scaled version of the amount of time that  $Z^r$  spends on the boundary. In our diffusion approximation, we approximate this by a continuous non-decreasing process  $\tilde{L}^r$  that can increase only when our diffusion process is on the boundary  $\widehat{G}^{b,r}$ . Indeed, in [27], under certain conditions, a more extensive rationale is given for approximating  $L^r$  by  $\tilde{L}^r$ . This involves showing that if the jump size  $\delta = \frac{1}{\sqrt{r}}$  in  $Y_k^r$  is sent to zero and at the same time the order of magnitude of the speed of jumping,  $\delta^{-2} = r$ , is sent to infinity, while keeping the other  $r$  dependencies fixed, then  $L^r$  converges (weakly) to the process  $\tilde{L}^r$ .

This leads us to propose the following equation for our diffusion approximation  $\tilde{Z}^r$  for  $\overline{X}^r$ :

$$\tilde{Z}^r(t) = \tilde{Z}^r(0) + \int_0^t \mu(\tilde{Z}^r(s)) ds + \frac{1}{\sqrt{r}} \int_0^t \sigma(\tilde{Z}^r(s)) dW(s) + \frac{1}{\sqrt{r}} \int_0^t \gamma(\tilde{Z}^r(s)) d\tilde{L}^r(s), \quad (33)$$

where  $\tilde{Z}^r$  is a continuous process living in  $\widehat{G}^r$  and  $\tilde{L}^r$  is a continuous, one-dimensional, increasing process that starts from zero and that can only increase when  $\tilde{Z}^r$  is on the boundary  $\widehat{G}^{b,r}$  of  $\widehat{G}^r$ . The vector field  $\gamma$  defines the “reflection” vector field on the boundary for the process  $\tilde{Z}^r$ . This is the direction in which  $\tilde{Z}^r$  is “pushed” to keep it in the set  $\widehat{G}^r$ . The process  $\tilde{L}^r$  is the cumulative amount of “pushing” done at the boundary. For more detail on reflected diffusion processes see Appendix A.

In [27], Leite and Williams prove well posedness of equation (33), under the assumption that the reaction network satisfies a mass-conserving (or mass-dissipating) assumption, augmented by inflows and outflows on all species. The latter means that the reactions



are part of the set of reactions for each  $i = 1, \dots, m$ <sup>7</sup>. Systems without some of these inflow/outflow reactions can be approximated by including such reactions with very small rate constants  $c_k$ , so that the reactions rarely occur. If one does not make this assumption, issues regarding existence and uniqueness of the diffusion process can arise. These are related to the fact that  $\sigma$  might only be Hölder continuous near the boundary in some places, the vector field  $\gamma$  on the boundary might degenerate to either become zero or not point strictly into the interior of the state space  $\hat{G}^r$  at some places on  $\hat{G}^{b,r}$ . The mass-conserving/mass-dissipating assumption, in combination with outflows on all species, is used to ensure non-explosion of the diffusion process. These assumptions can sometimes be relaxed, especially when  $\hat{G}^r$  is one-dimensional (or effectively so, as in Example 2), and in some cases in higher dimensions, if one can show that problematical boundary regions are not reached by the diffusion and there is no explosion in finite time. However, a systematic treatment of these matters requires new developments for the theory of reflected diffusions in polyhedral domains with degenerate dispersion coefficients and reflection vector fields. Nevertheless, we conjecture that a process  $\tilde{Z}^r$  satisfying (33) will be a good approximation to  $\bar{X}^r$ , whenever the former is well defined. In the next section, we give examples that illustrate how well our diffusion approximation works, despite the informal nature of our derivation. Further examples can be found in [27]<sup>8</sup>.

A problem for further investigation is to develop estimates of the error between  $\bar{X}^r$  and  $\tilde{Z}^r$ , assuming the latter is well defined. While this can be done when  $\tilde{Z}^r$  is one-dimensional, a systematic treatment of this is a promising area for future investigation.

## 4 Examples

We begin this section by showing how the stationary distributions for the constrained Langevin approximation can be computed for the two examples given in Section 3.1. The results are then compared with the stationary distributions for the Markov chain model and for the linear noise approximation. Later, in Section 4.2, we further illustrate the constrained Langevin approximation by comparing its simulation for some two-dimensional examples with those for the Markov chain model, the linear noise approximation, and the complex Langevin approximation introduced in [33].

### 4.1 Stationary distributions

The approximations proposed in Section 3 are for stochastic processes over compact time intervals. In this subsection we look for insights into the long time behavior by considering stationary distributions for some examples where analytical expressions are available.

**Example 1 (revisited).** We begin by noting that for a fixed  $r > 0$ , the stationary distribution of the (scaled) jump model (13) satisfies [1]:

$$\pi(x) = e^{-r\alpha/\beta} \frac{(r\alpha/\beta)^{rx}}{(rx)!}, \quad x \in \left\{0, \frac{1}{r}, \frac{2}{r}, \dots\right\}. \quad (35)$$

Turning to our constrained Langevin approximation, by (17) and Itô's formula [9], for  $f \in C_c^2([0, \infty))$

<sup>7</sup>This assumption ensures that  $\sigma$  is strictly positive definite and locally Lipschitz continuous on  $\hat{G}^r = \mathbb{R}_{\geq 0}^m$ , that  $\gamma$  never vanishes on  $\hat{G}^{b,r}$  and it points strictly in to the interior of  $\hat{G}^r$ . As shown in [27], the conditions given there are sufficient to prove existence, uniqueness and non-explosion of the diffusion process  $\tilde{Z}^r$ .

<sup>8</sup>It is also shown in [27], under mild conditions, that a sequence of jump-diffusion processes, in which the jumps at the boundary are allowed to shrink to zero at the same time that the rate of jumping goes to infinity, converges weakly to a solution of (33).

(two times continuously differentiable functions with compact support),

$$\begin{aligned} f(\tilde{Z}^r(t)) - f(\tilde{Z}^r(0)) &= \int_0^t (\alpha - \beta \tilde{Z}^r(s)) f'(\tilde{Z}^r(s)) ds + \frac{1}{\sqrt{r}} \int_0^t \sqrt{\alpha + \beta \tilde{Z}^r(s)} f'(\tilde{Z}^r(s)) d\tilde{W}(s) \\ &\quad + \frac{1}{2r} \int_0^t (\alpha + \beta \tilde{Z}^r(s)) f''(\tilde{Z}^r(s)) ds + \frac{1}{\sqrt{r}} \int_0^t f'(\tilde{Z}^r(s)) d\tilde{Y}^r(s). \end{aligned}$$

Suppose now that  $f'(0) = 0$ . Then the last term is zero because  $\tilde{Y}^r$  can only increase when  $\tilde{Z}^r$  is at zero. The integral with respect to  $d\tilde{W}$  defines a martingale and so, taking expectations when  $\tilde{Z}^r(0)$  has the stationary distribution  $\pi$  with density  $\rho$ , we obtain

$$0 = \int_0^t E_\pi [\mathcal{L}f(\tilde{Z}^r(s))] ds \quad \text{for all } t \geq 0,$$

where

$$\begin{aligned} (\mathcal{L}f)(x) &= (\alpha - \beta x) f'(x) + \frac{1}{2r} (\alpha + \beta x) f''(x) \\ &= \mu(x) f'(x) + \frac{1}{2r} \Upsilon(x) f''(x), \end{aligned}$$

for  $\mu(x) = \alpha - \beta x$  and  $\Upsilon(x) = \alpha + \beta x$ . Hence  $\rho$  must satisfy

$$\int_0^\infty (\mathcal{L}f)(x) \rho(x) dx = 0, \quad \int_0^\infty \rho(x) dx = 1. \quad (36)$$

Integration by parts yields

$$\begin{aligned} \int_0^\infty (\mathcal{L}f)(x) \rho(x) dx &= \int_0^\infty f(x) \left( \frac{1}{2r} \frac{d^2}{dx^2} [\Upsilon(x) \rho(x)] - \frac{d}{dx} [\mu(x) \rho(x)] \right) dx \\ &\quad - f(0) \left( \mu(0) \rho(0) - \frac{1}{2r} \frac{d}{dx} (\Upsilon(x) \rho(x)) \Big|_{x=0} \right), \end{aligned}$$

where we have used the facts that  $f'(0) = 0$  and  $f$  has compact support in the above calculation. As the above must hold for all  $f \in C_c^2([0, \infty))$  with  $f'(0) = 0$ , we see that  $\rho$  must satisfy

$$(\mathcal{L}^* \rho)(x) = -\frac{d}{dx} (\mu(x) \rho(x)) + \frac{1}{2r} \frac{d^2}{dx^2} (\Upsilon(x) \rho(x)) = 0, \quad \text{for all } x \in (0, \infty), \quad (37)$$

where  $\mathcal{L}^*$  denotes the adjoint of  $\mathcal{L}$ , with the boundary condition

$$\left( \mu \rho - \frac{1}{2r} \frac{d}{dx} (\Upsilon \rho) \right) \Big|_{x=0} = 0. \quad (38)$$

Integrating (37) shows that

$$-\mu(x) \rho(x) + \frac{1}{2r} \frac{d}{dx} (\Upsilon(x) \rho(x)) = 0, \quad \text{for all } x \geq 0, \quad (39)$$

where the value of zero on the right hand side follows from the boundary condition (38). Solving equation (39), noting that  $\Upsilon(x) > 0$  for all  $x \geq 0$ , yields

$$\rho(x) = \frac{c}{\Upsilon(x)} \exp \left\{ \int_0^x \frac{2r\mu(s)}{\Upsilon(s)} ds \right\}, \quad \text{for } x \geq 0, \quad (40)$$



where  $c$  is a suitable normalizing constant. After substituting for our specific  $\mu$  and  $\Upsilon$ , we obtain

$$\rho(x) = ce^{-2xr} (\alpha + \beta x)^{(4r\alpha/\beta)-1}, \quad \text{for } x \geq 0, \quad (41)$$

where

$$c = \left( \int_0^\infty e^{-2xr} (\alpha + \beta x)^{(4r\alpha/\beta)-1} dx \right)^{-1}, \quad (42)$$

is the normalizing constant.

The linear noise approximation [40] for the Markov chain  $\bar{X}_1^r$  has as its stationary distribution,  $\rho_{LN}$ , the steady-state distribution for the Ornstein-Uhlenbeck type process  $\hat{Z}_1^r$  that describes the linearized fluctuations of  $\bar{X}_1^r$  about  $\bar{x} = \frac{\alpha}{\beta}$ , the (stable) steady-state for the deterministic reaction rate equation approximation to  $\bar{X}_1^r$  satisfying  $\mu(\bar{x}) = 0$ . This process  $\hat{Z}_1^r$  satisfies

$$\hat{Z}_1^r(t) = \bar{x} + \int_0^t \mu'(\bar{x})(\hat{Z}_1^r(s) - \bar{x}) ds + \frac{1}{\sqrt{r}} \int_0^t \sigma(\bar{x}) d\hat{W}(s), \quad (43)$$

where  $\mu'(\bar{x}) = -\beta$ ,  $\sigma(\bar{x}) = \sqrt{\Upsilon(\bar{x})} = \sqrt{\alpha + \beta\bar{x}} = \sqrt{2\alpha}$  and  $\hat{W}$  is a standard one-dimensional Brownian motion. The stationary distribution for  $\hat{Z}_1^r$  is the Gaussian distribution with mean  $\frac{\alpha}{\beta}$  and variance  $\frac{\alpha}{r\beta}$  [40], so that

$$\rho_{LN}(x) = \sqrt{\frac{r\beta}{2\pi\alpha}} \exp\left(-\frac{r\beta(x - \frac{\alpha}{\beta})^2}{2\alpha}\right), \quad x \in (-\infty, \infty). \quad (44)$$

We now wish to compare the probability mass function in (35) with the densities in (41) and (44). Notice that the probability that a continuous model with strictly positive density function  $f$  takes a value in the interval  $[x - 1/(2r), x + 1/(2r))$  can be well approximated by  $f(x) \cdot r^{-1}$ . So in order to compare the density for the stationary distribution of the linear noise approximation with the stationary distribution of the Markov chain, we define  $\pi_{LN}(x) = \rho_{LN}(x) \cdot r^{-1}$  for  $x$  in the lattice  $(1/r)\mathbb{Z}$ , with  $\rho_{LN}$  as in (44). For the constrained Langevin approximation, we define the discretization  $\pi_{CLA}(x) = \rho(x) \cdot r^{-1}$  for  $x \in \{1/r, 2/r, \dots\}$ , with  $\rho$  as in (41). Since the density of the constrained Langevin approximation has no mass for  $x < 0$ , we let  $\pi_{CLA}(0) = \rho(0) \cdot r^{-1}/2$ , which is an approximation of the probability that the model takes a value in the interval  $[0, 1/(2r))$ . The result is shown in Figure 1 for the system with parameters  $\alpha = \beta = 1$  and  $r = 100$ . Note that  $\pi_{LN}$  is defined for all  $x$ , whereas  $\pi$  and  $\pi_{CLA}$  are only defined for  $x \geq 0$ .

**Example 2 (revisited).** For fixed  $r > 0$ , the stationary distribution of the (scaled) Markov chain jump model (20) satisfies

$$\pi(x) = \pi(0) \left( \frac{\beta_2}{\beta_1} \right)^{rx} \frac{(M^r + 1 - rx)(M^r + 2 - rx) \cdots M^r}{(rx)!}, \quad \text{for } x \in \left\{ \frac{1}{r}, \frac{2}{r}, \dots, \bar{M}^r \right\}, \quad (45)$$

where  $\pi(0)$  is determined so that  $\sum_{x=0}^{\bar{M}^r} \pi(x) = 1$ .

Turning to our constrained Langevin approximation, the density function  $\rho$  of the stationary distribution for  $\hat{Z}_1^r$ , satisfying (24), is supported on  $[0, \bar{M}^r]$  and, similarly to how (36) was derived, must satisfy the following two conditions [22]:

$$\int_0^{\bar{M}^r} (\mathcal{L}f)(x) \rho(x) dx = 0, \quad \int_0^{\bar{M}^r} \rho(x) dx = 1,$$

for all  $f \in C^2([0, \bar{M}^r])$  satisfying  $f'(0) = f'(\bar{M}^r) = 0$ , where

$$\begin{aligned} (\mathcal{L}f)(x) &= (\beta_2 \bar{M}^r - (\beta_1 + \beta_2)x) f'(x) + \frac{1}{2r} (\beta_2 \bar{M}^r + (\beta_1 - \beta_2)x) f''(x) \\ &= \mu(x) f'(x) + \frac{1}{2r} \Upsilon(x) f''(x), \end{aligned}$$

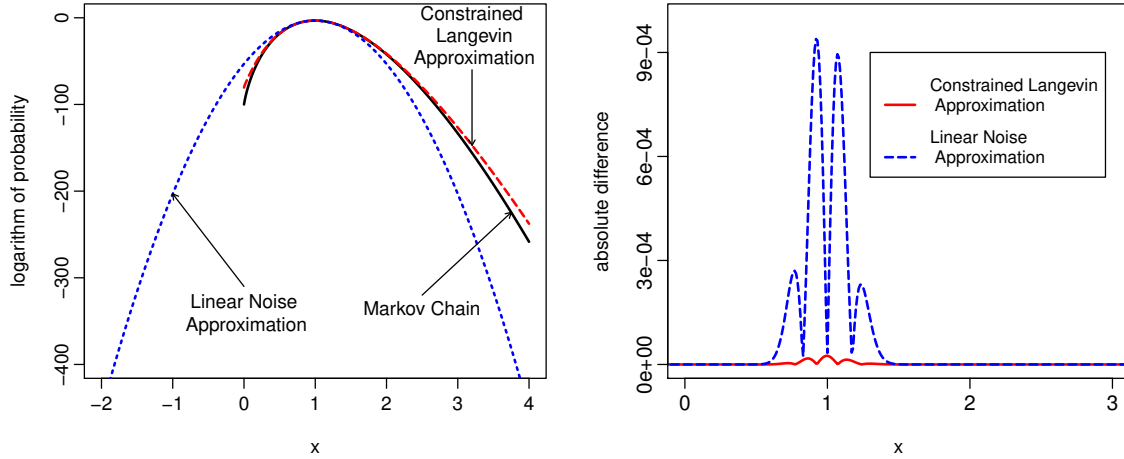


Figure 1: (Left) Comparison of  $\log(\pi(x))$ ,  $\log(\pi_{CLA}(x))$ , and  $\log(\pi_{LN}(x))$ , where  $\log(\cdot)$  denotes the natural logarithm, for Example 1 with  $\alpha = \beta = 1$  and  $r = 100$ . (Right) Absolute difference between the stationary distribution for the Markov chain and those given by the constrained Langevin and linear noise approximations (i.e.,  $|\pi_{CLA}(x) - \pi(x)|$  and  $|\pi_{LN}(x) - \pi(x)|$ ). Values of  $x$  are taken from the lattice  $(1/r)\mathbb{Z}$  and linear interpolation is used to connect the values.

for  $\mu(x) = \beta_2 \overline{M}^r - (\beta_1 + \beta_2)x$  and  $\Upsilon(x) = \beta_2 \overline{M}^r + (\beta_1 - \beta_2)x$ . Here, to simplify notation, we have suppressed the explicit dependence of  $\mu$  and  $\Upsilon$  on  $r$  (which occurs through  $\overline{M}^r$ ). Integration by parts gives

$$\begin{aligned} \int_0^{\overline{M}^r} (\mathcal{L}f)(x)\rho(x)dx &= \int_0^{\overline{M}^r} f(x) \left( \frac{1}{2r} \frac{d^2}{dx^2} [\Upsilon(x)\rho(x)] - \frac{d}{dx} [\mu(x)\rho(x)] \right) dx \\ &\quad + \left[ f \left( \mu\rho - \frac{1}{2r} \frac{d}{dx} (\Upsilon\rho) \right) \right]_{x=0}^{\overline{M}^r}. \end{aligned}$$

Therefore, as the above must hold for all such  $f$ , we must have

$$(\mathcal{L}^* \rho)(x) = -\frac{d}{dx}(\mu(x)\rho(x)) + \frac{1}{2r} \frac{d^2}{dx^2}(\Upsilon(x)\rho(x)) = 0, \quad \text{for all } x \in (0, \overline{M}^r), \quad (46)$$

where  $\mathcal{L}^*$  is the adjoint of  $\mathcal{L}$ , and

$$\left( \mu\rho - \frac{1}{2r} \frac{d}{dx} (\Upsilon\rho) \right) \Big|_{x=0} = \left( \mu\rho - \frac{1}{2r} \frac{d}{dx} (\Upsilon\rho) \right) \Big|_{x=\overline{M}^r} = 0. \quad (47)$$

Integrating (46) gives

$$-\mu(x)\rho(x) + \frac{1}{2r} \frac{d}{dx}(\Upsilon(x)\rho(x)) = 0, \quad \text{for all } x \in [0, \overline{M}^r], \quad (48)$$

where the value of zero on the right hand side follows from the boundary conditions (47). Solving equation (48) yields a solution of the form (40), which after substituting for our specific  $\mu$  and  $\Upsilon$  becomes

$$\rho(x) = \begin{cases} c \exp \left\{ -\frac{2(\beta_1 + \beta_2)}{\beta_1 - \beta_2} rx \right\} (\beta_2 \overline{M}^r + (\beta_1 - \beta_2)x)^{-1 + \frac{4\overline{M}^r r \beta_1 \beta_2}{(\beta_1 - \beta_2)^2}}, & \text{if } \beta_1 \neq \beta_2, \\ c \exp \left\{ -\frac{(x - \frac{1}{2}\overline{M}^r)^2}{\overline{M}^r / 2r} \right\}, & \text{if } \beta_1 = \beta_2, \end{cases} \quad (49)$$

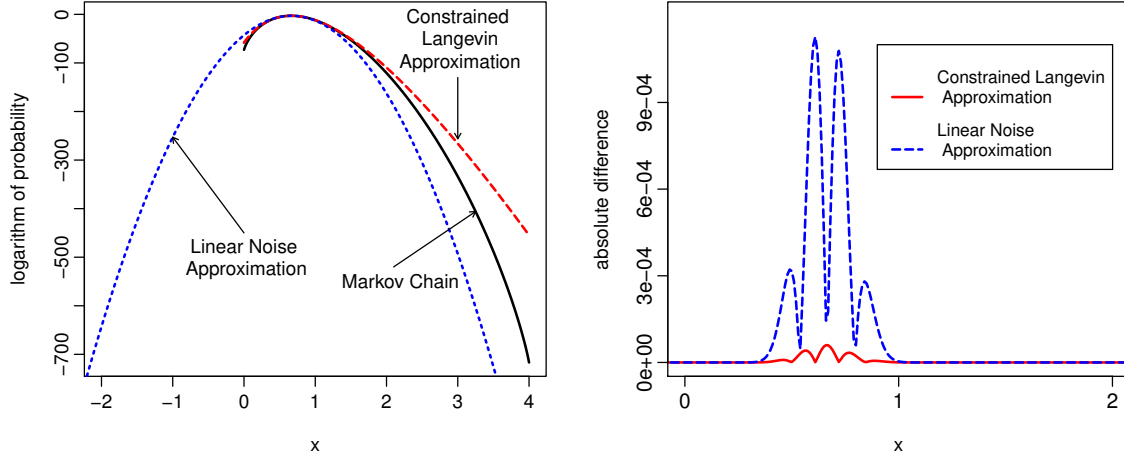


Figure 2: (Left) Comparison of  $\log(\pi(x))$ ,  $\log(\pi_{CLA}(x))$ , and  $\log(\pi_{LN}(x))$ , where  $\log(\cdot)$  denotes the natural logarithm, for Example 2 with  $\beta_1 = 5$  and  $\beta_2 = 1$ ,  $M^r = 400$  and  $r = 100$ . (Right) Absolute difference between the stationary distribution for the Markov chain and those given by the constrained Langevin and linear noise approximations (i.e.,  $|\pi_{CLA}(x) - \pi(x)|$  and  $|\pi_{LN}(x) - \pi(x)|$ ). Values of  $x$  are taken from the lattice  $(1/r)\mathbb{Z}$  and linear interpolation is used to connect the values.

for  $0 \leq x \leq \overline{M}^r$ , where  $c$  is the normalizing constant chosen so that  $\int_0^{\overline{M}^r} \rho(x) dx = 1$ . Note that in the case of  $\beta_1 = \beta_2$ , the stationary distribution is a Gaussian distribution restricted to  $[0, \overline{M}^r]$ .

The linear noise approximation [40] for the Markov chain  $\overline{X}_1^r$  in this example has as its stationary distribution,  $\rho_{LN}$ , the steady-state distribution for the Ornstein-Uhlenbeck type process  $\hat{Z}_1^r$  that describes the linearized fluctuations of  $\overline{X}_1^r$  about  $\bar{x} = \frac{\beta_2 \overline{M}^r}{\beta_1 + \beta_2}$ , the (stable) steady-state for the deterministic reaction rate equation approximation to  $\overline{X}_1^r$  satisfying  $\mu(\bar{x}) = 0$ . This process  $\hat{Z}_1^r$  satisfies

$$\hat{Z}_1^r(t) = \bar{x} + \int_0^t \mu'(\bar{x})(\hat{Z}_1^r(s) - \bar{x}) ds + \frac{1}{\sqrt{r}} \int_0^t \sigma(\bar{x}) d\hat{W}(s) \quad (50)$$

where  $\mu'(\bar{x}) = -(\beta_1 + \beta_2)$ ,  $\sigma(\bar{x}) = \sqrt{\Upsilon(\bar{x})} = \sqrt{\beta_2 \overline{M}^r + (\beta_1 - \beta_2)\bar{x}} = \sqrt{\frac{2\beta_1\beta_2\overline{M}^r}{\beta_1 + \beta_2}}$  and  $\hat{W}$  is a standard one-dimensional Brownian motion. The stationary distribution for  $\hat{Z}_1^r$  is the Gaussian distribution with mean  $\bar{x} = \frac{\beta_2 \overline{M}^r}{\beta_1 + \beta_2}$  and variance  $\frac{\Upsilon(\bar{x})}{2r|\mu'(\bar{x})|} = \frac{\beta_1\beta_2\overline{M}^r}{r(\beta_1 + \beta_2)^2}$  [40], so that

$$\rho_{LN}(x) = \sqrt{\frac{r}{2\pi\beta_1\beta_2\overline{M}^r}}(\beta_1 + \beta_2) \exp\left(-\frac{r(\beta_1 + \beta_2)^2 \left(x - \frac{\beta_2 \overline{M}^r}{\beta_1 + \beta_2}\right)^2}{2\beta_1\beta_2\overline{M}^r}\right), \quad x \in (-\infty, \infty). \quad (51)$$

In a similar manner to that for the previous example, we want to compare the probability mass function in (45) with the densities in (49) and (51). Again, in order to compare the density for the stationary distribution of the linear noise approximation with the stationary distribution of the Markov chain, we define  $\pi_{LN}(x) = \rho_{LN}(x) \cdot r^{-1}$  for  $x$  in the lattice  $(1/r)\mathbb{Z}$ , with  $\rho_{LN}$  as in (51). For the constrained Langevin approximation, we define the discretization  $\pi_{CLA}(x) = \rho(x) \cdot r^{-1}$  for  $x \in \{1/r, 2/r, \dots, \overline{M}^r - 1/r\}$ , with  $\rho$  as in (49) and, since the density of the constrained Langevin approximation has no mass for  $x < 0$  or for  $x > \overline{M}^r$ , we let  $\pi_{CLA}(0) = \rho(0) \cdot r^{-1}/2$  and  $\pi_{CLA}(\overline{M}^r) = \rho(\overline{M}^r) \cdot r^{-1}/2$ , which is an approximation of the probability

that the model takes a value in the interval  $[0, 1/(2r))$  and  $[\overline{M}^r - 1/(2r), \overline{M}^r]$ , respectively. The result is shown in Figure 2 for the system with parameters  $\beta_1 = 5$ ,  $\beta_2 = 1$ ,  $\overline{M}^r = 400$  and  $r = 100$ . Note that  $\pi_{LN}$  is defined for all  $x$ , whereas  $\pi$  and  $\pi_{CLA}$  are only defined for  $0 \leq x \leq \overline{M}^r$ .

For the cases illustrated in Figures 1 and 2, we see that, in addition to having the correct support, the stationary distribution for the constrained Langevin approximation captures the behavior of the Markov chain model more accurately than the linear noise approximation.

## 4.2 Simulation examples

**Example 3.** We now consider a chemical reaction system involving two molecular species  $S_1$  and  $S_2$  with the following set of reactions:



This reaction set is a simple mass-action kinetic system whose reaction rate equation (deterministic model) exhibits a limit cycle [32]. For this example, the constrained Langevin approximation, given by equation (33), has drift and diffusion matrix given by:

$$\mu(x) = \begin{pmatrix} \nu x_1^2 x_2 - \beta_1 x_1 + \alpha_1 \\ -\nu x_1^2 x_2 - \beta_2 x_2 + \alpha_2 \end{pmatrix}, \quad \Upsilon(x) = \begin{pmatrix} \nu x_1^2 x_2 + \beta_1 x_1 + \alpha_1 & -\nu x_1^2 x_2 \\ -\nu x_1^2 x_2 & \nu x_1^2 x_2 + \beta_2 x_2 + \alpha_2 \end{pmatrix},$$

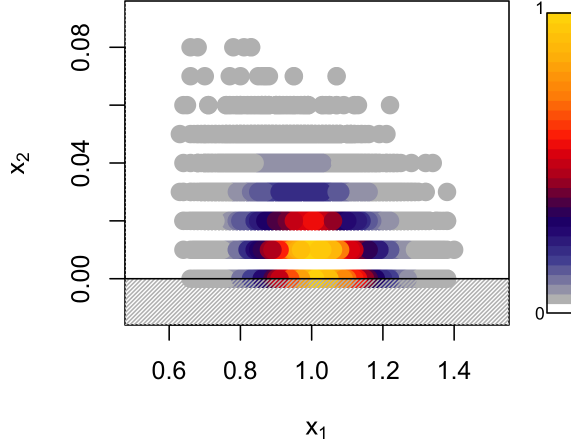
and the reflection vector field is given by

$$\gamma(x) = \begin{cases} \begin{pmatrix} \alpha_1 \\ \alpha_2 - \beta_2 x_2 \end{pmatrix} / \sqrt{\alpha_1^2 + (\alpha_2 - \beta_2 x_2)^2}, & \text{for } x_1 = 0 \\ \begin{pmatrix} \alpha_1 - \beta_1 x_1 \\ \alpha_2 \end{pmatrix} / \sqrt{(\alpha_1 - \beta_1 x_1)^2 + \alpha_2^2}, & \text{for } x_2 = 0. \end{cases} \quad (53)$$

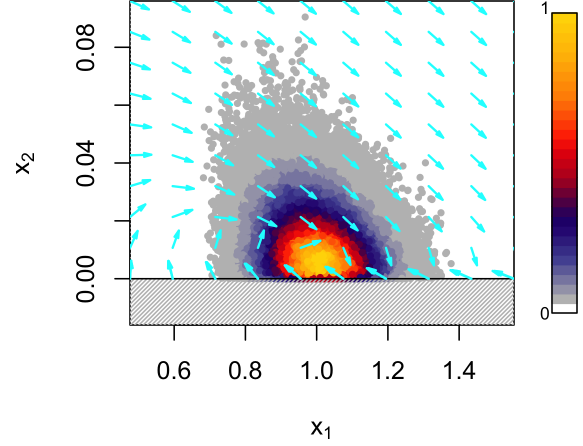
We compare the constrained Langevin approximation (CLA) with the Markov chain (MC) model, the linear noise approximation (LNA), and a Langevin equation with normal reflection at the boundaries (LEN). That is, LEN is given as in equation (33) with the exception that the direction of reflection is normal to the boundary. The MC model was simulated using Gillespie's Algorithm (or SSA) [16]. For the LNA, we used a fourth order Runge-Kutta method for the deterministic part and the Euler-Maruyama method for the stochastic diffusion. For the CLA and LEN, we used Bossy et al.'s algorithm [8], which is a numerical method for simulating obliquely reflected stochastic differential equations based on the Euler-Maruyama method. The simulation codes were written in the R programming language [30].

We consider two sets of parameters for this reaction system. First, we set  $r = 100$ ,  $\nu = 10$ ,  $\beta_1 = 0.2$ ,  $\beta_2 = 10^{-9}$  and  $\alpha_1 = \alpha_2 = 0.1$ . For this choice, the reaction rate equation does not exhibit a limit cycle, but it spends most of its time near the boundary  $x_2 = 0$ . The time step for the numerical methods used for the diffusion approximations and the deterministic reaction rate equation were set to  $h = 0.01$  and the simulations were performed up to time  $T = 10^4$ . The simulations were initialized at the stationary point for the deterministic model. Figure 3 shows the scatter plot of the points generated by the simulations. For the CLA and the LEN, we also display the reflection directions at the boundary and the drift vector field inside the state-space, which is normalized to have unit length to improve the display. Notice that the LNA permits negative concentrations. In addition, LEN produces a shift to the right due to the effect of the normal reflection directions. Such a shift is not seen in the CLA simulation, since the reflection on  $x_2 = 0$  is oblique, pointing towards the left of the plot.

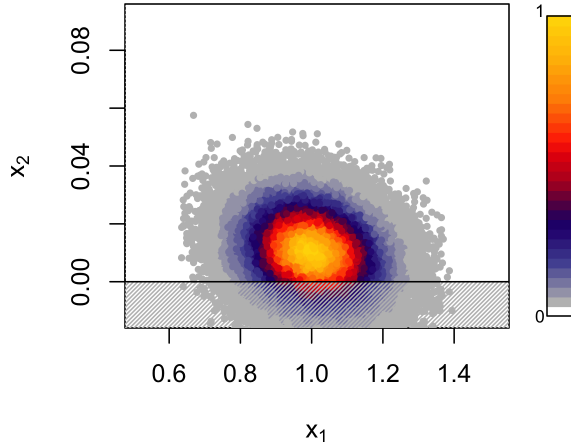
In order to have a more precise measure of error, we estimate a discrete density for each of the simulations. This density estimation is calculated by dividing the state space into a regular grid of square bins and



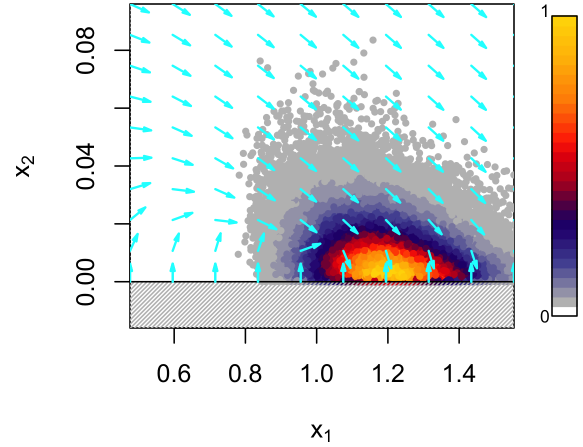
(a) Markov Chain (MC)



(b) Constrained Langevin Approximation (CLA)



(c) Linear Noise Approximation (LNA)



(d) Langevin with Normal Reflection (LEN)

Figure 3: Scatter plot of the concentrations of  $S_1$  and  $S_2$ , given by  $x_1$  and  $x_2$ , respectively, generated from simulations of the MC, CLA, LNA and LEN for the system given by (52) with parameters  $r = 100$ ,  $\nu = 10$ ,  $\beta_1 = 0.2$ ,  $\beta_2 = 10^{-9}$ , and  $\alpha_1 = \alpha_2 = 0.1$ . For the Markov chain, the plotted points were magnified in order to improve the display, since the values are within the lattice  $(1/r)\mathbb{Z}^2$ . For (b) CLA and (d) LEN we also show the directions of reflection at the boundary  $x_2 = 0$  and the normalized drift vector field inside the state space. Notice that the distribution of points for (d) LEN is shifted to the right from the other plots, due to the normal reflection, and that (c) LNA permits negative concentrations for  $S_2$ .

counting the number of simulation points present in each of these bins. These square bins have a side length of  $1/r$  and are centered around each state of the Markov chain model. The total number of points inside each square bin is normalized by the total number of points in the simulation and the area of the square. In order to measure statistical variation among different simulation runs, the experiment was repeated 10 times, using the same data from the previous paragraph. Table 1 shows the integral (with respect to Lebesgue measure) of the absolute difference between the discrete density calculated for the Markov chain simulation and those generated by the simulation of each approximation. Notice that the maximum possible value for these integrals is 2.

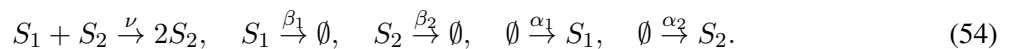
Table 1: Integral of the absolute difference between the discrete densities calculated for the approximation processes and that for the Markov chain simulation (for parameters as in Figure 3). The values displayed are averages of 10 independent runs. The 95% confidence intervals for these averages are also shown.

	Integral of Absolute Difference	95% C. I.
Linear Noise Approximation (LNA)	0.2762	(0.2716, 0.2808)
Constrained Langevin Approximation (CLA)	0.2432	(0.2373, 0.2490)
Langevin with Normal Reflection (LEN)	1.1710	(1.1529, 1.1892)

For the second set of parameters, we let  $r = 100$ ,  $\nu = 1$ ,  $\beta_1 = 1$ ,  $\beta_2 = 10^{-9}$ ,  $\alpha_1 = 0.1$  and  $\alpha_2 = 0.5$ . This time, the reaction rate equation for this system exhibits a limit cycle which lives near the boundaries  $x_1 = 0$  and  $x_2 = 0$ . For this example, we used a time step of  $h = 0.1$  for the numerical methods, simulations were performed up to time  $T = 10^5$ , and the initial condition was set to  $x^0 = (1, 1)$ . The scatter plots for the simulations of MC and CLA are shown in Figure 5. The paths generated by the simulations of LNA and LEN grow without bound. For this reason, the scatter plots for these simulations are not shown. For the LNA, this divergence occurs despite the fact that the deterministic part of the model exhibits a stable limit cycle. This type of behavior of the LNA is known [34, 38, 41]. Although some corrective measures have been proposed for similar examples (see [29] and references therein), this illustrates the incapability of LNA to characterize non-linear behavior adequately. From Figure 4, we see that the path generated by the simulation of the LEN becomes unstable after it hits a reflection from the boundary  $x_2 = 0$ , which is normal and pushes the process towards higher concentrations of  $x_1$ , as can be seen from the vector field of Figure 5(b). This path is reflected again (perpendicularly) from the  $x_2 = 0$  boundary, making the concentration of  $x_1$  increasingly larger, which leads to numerical instability and divergence for the chosen step size.

Similarly to the previous example, a discrete density estimation was calculated for the constrained Langevin approximation (it was not possible to perform this calculation for the Langevin with normal reflection and the linear noise approximations since these simulations diverge). The integral of the absolute difference between the discrete density calculated for the constrained Langevin approximation and that for the Markov chain was given by 0.3058 with a 95% confidence interval of (0.3044, 0.3072) among the 10 independent runs.

**Example 4.** Now we consider a different example in order to compare the constrained Langevin approximation proposed here with the complex Langevin approximation introduced in [33]. The examples in [33] involve unimolecular and bimolecular reactions. Here, we consider the following example involving such reactions for species  $S_1$  and  $S_2$ :





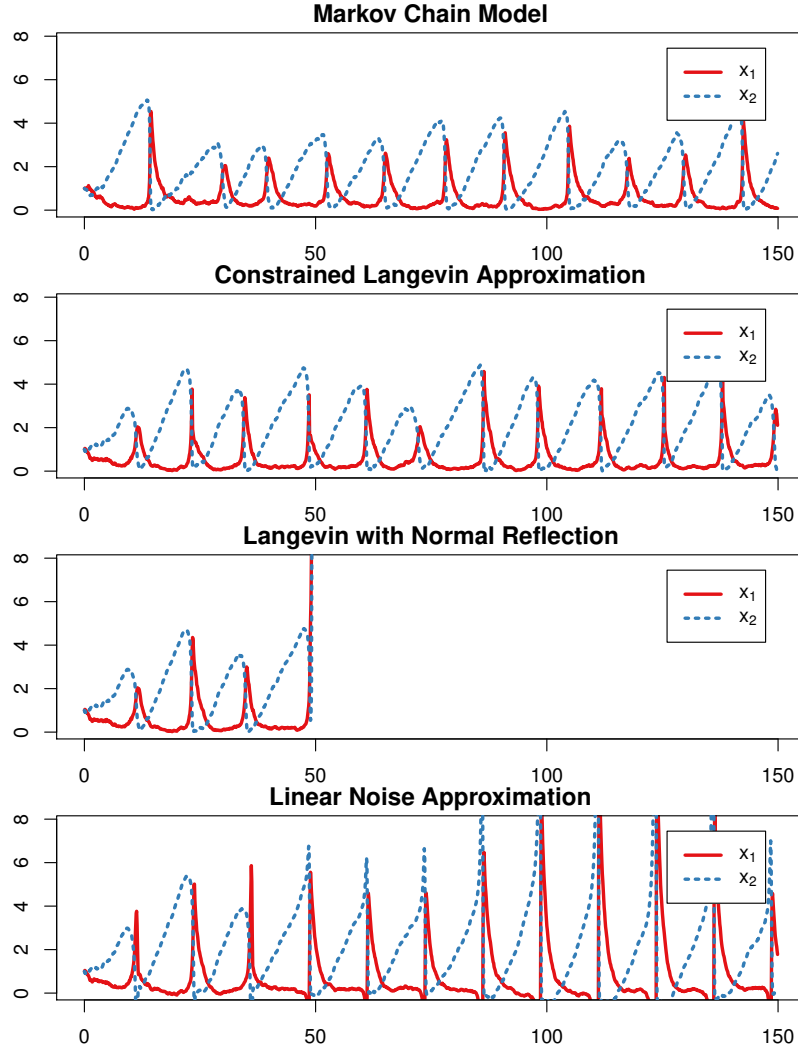


Figure 4: Plot of the concentrations of  $S_1$  and of  $S_2$  given by  $x_1$  and  $x_2$ , respectively, versus time. The paths were generated from simulations for the system given by (52) with parameters  $r = 100$ ,  $\nu = 1$ ,  $\beta_1 = 1$ ,  $\beta_2 = 10^{-9}$ ,  $\alpha_1 = 0.1$  and  $\alpha_2 = 0.5$ . Here we see that the LNA is unstable from early on in the simulation and that the LEN hits an unstable path near  $t = 50$ , where the normal reflection at the level  $x_2 = 0$  pushes the process to take a path with increasingly higher concentrations of  $x_1$ , leading the simulation to diverge.

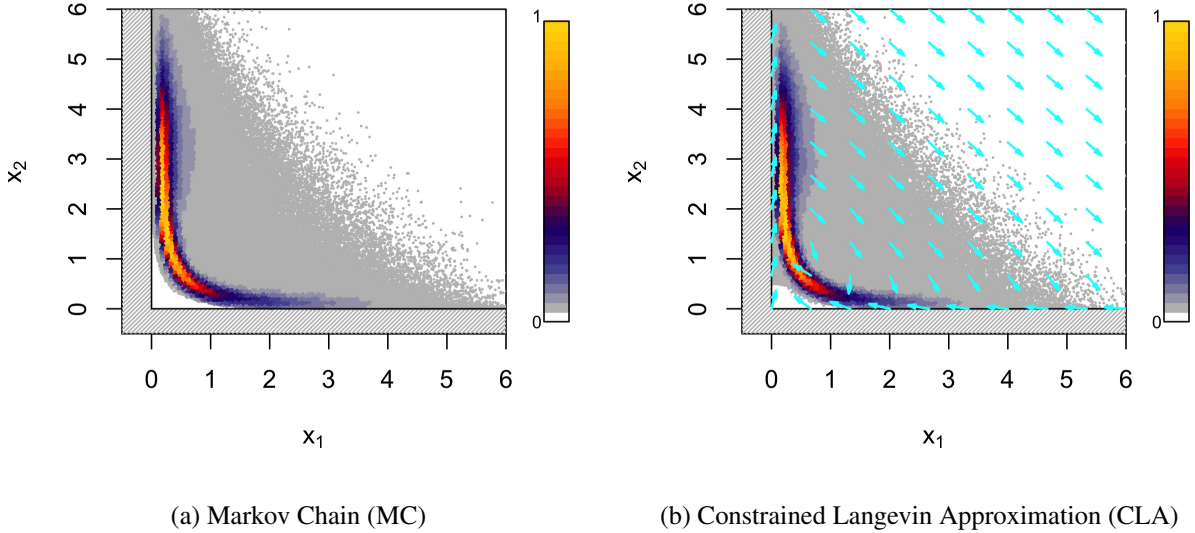


Figure 5: Scatter plot of the concentrations of  $S_1$  and  $S_2$ , given by  $x_1$  and  $x_2$ , respectively, generated from simulations of the MC and CLA for the system given by (52) with parameters  $r = 100$ ,  $\nu = 1$ ,  $\beta_1 = 1$ ,  $\beta_2 = 10^{-9}$ ,  $\alpha_1 = 0.1$  and  $\alpha_2 = 0.5$ . For (b), for the CLA, we show the reflection directions at the boundaries used by the approximation and the normalized drift vector field. The paths for the LNA and LEN generated by simulation diverge from the limit cycle and are not shown here.

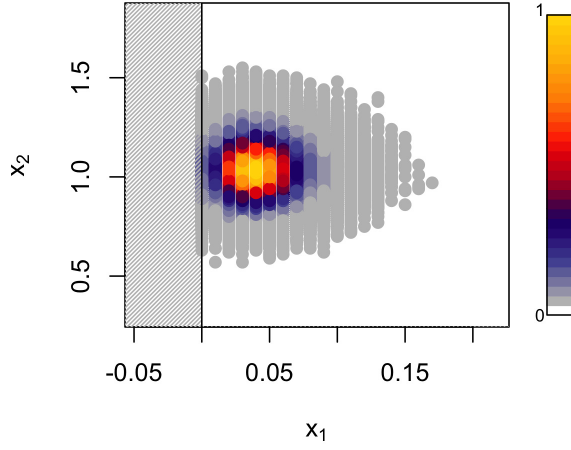
The drift and diffusion matrix of the constrained Langevin approximation for this example is given by

$$\mu(x) = \begin{pmatrix} -\nu x_1 x_2 - \beta_1 x_1 + \alpha_1 \\ \nu x_1 x_2 - \beta_2 x_2 + \alpha_2 \end{pmatrix}, \quad \Upsilon(x) = \begin{pmatrix} \nu x_1 x_2 + \beta_1 x_1 + \alpha_1 & -\nu x_1 x_2 \\ -\nu x_1 x_2 & \nu x_1 x_2 + \beta_2 x_2 + \alpha_2 \end{pmatrix},$$

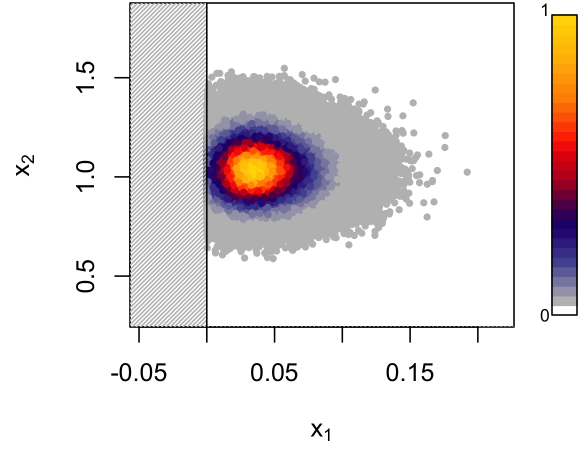
with the reflection vector field at the boundary given by (53), since on the boundaries  $x_1 = 0$  and  $x_2 = 0$ , the reflection vector field for (52) is the same as for (54).

Simulations were performed for the Markov chain model (MC), constrained Langevin approximation (CLA), the linear noise approximation (LNA), and the complex Langevin approximation (Complex-LE). We used the Euler-Maruyama method for the Complex-LE, similarly to what was done in [33], and we used Bossy et al.'s method [8] for the CLA. For the LNA, we used a fourth order Runge-Kutta method for its deterministic part and the Euler-Maruyama for its diffusion part. The simulations were performed up to time  $T = 10^5$  and the time steps for the numerical methods were set to  $h = 0.01$ . The initial condition used for the simulations was set to  $x_0 = (1, 1)/r$ , with  $r = 100$ , and the samples from the simulations were collected after an initial time of duration one was completed.

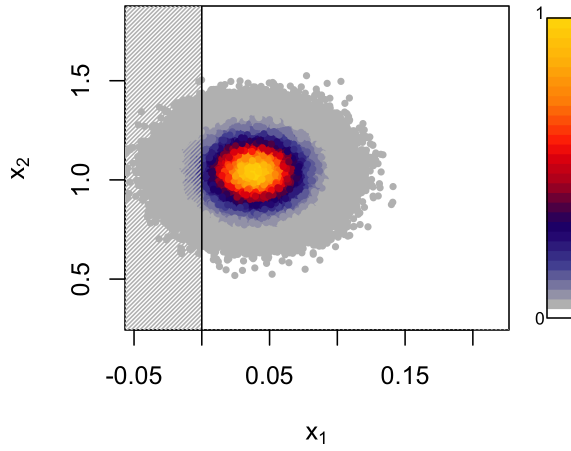
Since the Complex-LE predicts real-valued moments, we compare the approximations by calculating mean concentration values, their variances and covariance. In order to account for statistical variation among different runs and calculate confidence intervals, we repeated the simulations 10 times. Table 2 gives the results for the parameters  $r = 100$ ,  $\nu = \alpha_1 = \alpha_2 = \beta_2 = 1$  and  $\beta_1 = 25$ . The predicted moments are fairly closely matched for all simulations. In Figure 6, we give the scatter plot for the simulations. For the complex Langevin approximation, only the real parts of the simulation points are shown. Although these simulation points appear to be similarly distributed to those in the Markov chain simulation, like the linear noise approximation, the real part of the complex Langevin approximation permits values outside of the positive orthant.



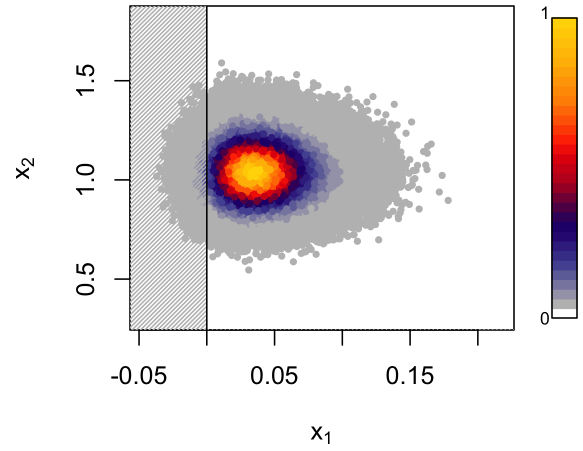
(a) Markov Chain (MC)



(b) Constrained Langevin Approximation (CLA)



(c) Linear Noise Approximation (LNA)



(d) Complex Langevin Approximation  
(Complex-LE)

Figure 6: Scatter plot of the concentrations of  $S_1$  and  $S_2$ , given by  $x_1$  and  $x_2$ , respectively, generated from simulations of the MC, CLA, LNA, and Complex-LE for the system given by (54) with parameters  $r = 100$ ,  $\nu = \alpha_1 = \alpha_2 = \beta_2 = 1$  and  $\beta_1 = 25$ . For the Complex-LE, only the real parts of the variables are shown. Notice that LNA and the Complex-LE predict negative values for  $x_1$  at some times.

Table 2: Means, variances and covariance for the concentration of each molecular species calculated by Markov chain (MC) simulation, the constrained Langevin approximations (CLA), the linear noise approximation (LNA), and the complex Langevin approximation (Complex-LE) (associated with the parameters as in Figure 6). The concentrations of species  $S_1$  and  $S_2$  are represented by  $x_1$  and  $x_2$ , respectively. The table displays the average values among 10 independent runs and also the value that should be added/subtracted to the mean to get the 95% confidence intervals.

	MC	CLA	LNA	Complex-LE
$E[x_1]$	3.854e-02 $\pm$ 3.29e-05	3.898e-02 $\pm$ 3.13e-05	3.836e-02 $\pm$ 5.03e-05	3.835e-02 $\pm$ 3.32e-05
$E[x_2]$	1.040e+00 $\pm$ 2.74e-04	1.040e+00 $\pm$ 3.41e-04	1.040e+00 $\pm$ 2.89e-04	1.040e+00 $\pm$ 2.68e-04
$\text{var}(x_1)$	3.839e-04 $\pm$ 1.08e-06	4.214e-04 $\pm$ 1.58e-06	4.408e-04 $\pm$ 1.10e-06	4.413e-04 $\pm$ 2.21e-06
$\text{var}(x_2)$	1.080e-02 $\pm$ 3.72e-05	1.070e-02 $\pm$ 3.95e-05	1.082e-02 $\pm$ 3.35e-05	1.086e-02 $\pm$ 3.78e-05
$\text{cov}(x_1, x_2)$	-1.582e-05 $\pm$ 5.30e-06	-1.924e-05 $\pm$ 3.36e-06	-1.603e-05 $\pm$ 4.25e-06	-1.857e-05 $\pm$ 3.69e-06

Since the real part of the complex Langevin approximation can take values outside of the positive orthant, its behavior depends on the values of the drift and dispersion coefficients there. We found that, for some examples, the drift vector field used by the complex Langevin approximation outside of the positive orthant can lead the process to have paths that diverge. One such example is found by considering the same example (54) with the following set of parameters  $r = 100$ ,  $\alpha_1 = \beta_1 = 1$ ,  $\nu = 10$ ,  $\alpha_2 = 0.02$ , and  $\beta_2 = 5$ . For this example, the simulation of the complex Langevin approximation using the Euler-Maruyama method diverges even with step sizes as small as  $h = 0.001$ . In order to illustrate this, we simulated the complex Langevin approximation with the time step  $h = 0.001$  up to time  $T = 10^5$ . The simulation hits a divergent path and stops at time  $t = 6665.421$ . Figure 7 shows the evolution of the real parts of the complex Langevin approximation for the molecular concentrations of species  $S_1$  and  $S_2$ , represented by variables  $x_1$  and  $x_2$ , respectively, prior to divergence. From this figure, we observe that the process has crossed the  $x_2 = 0$  boundary, where the drift vector field pushes the process to higher concentrations of  $x_1$  and negative values of  $x_2$ .

The same experiment was repeated for the Markov chain (MC), the constrained Langevin approximation (CLA), and the linear noise approximation (LNA), using the time step of  $h = 0.01$  for the numerical methods. The scatter plot for a simulation with duration  $T = 10^5$  is given in Figure 8. We also calculated the integral of the absolute difference between the discrete density calculated for the Markov chain and those calculated for the constrained Langevin and the linear noise approximations. The result is given in Table 3.

Table 3: Integral of the absolute difference between the discrete density calculated for the Markov chain simulation and those calculated for the constrained Langevin approximation and the linear noise approximation (for parameters as in Figure 8). The values displayed are averages of 10 independent runs. The 95% confidence intervals for these averages are also shown.

	Integral of Absolute Difference	95% C. I.
Constrained Langevin Approximation (CLA)	0.2299	(0.2283, 0.2315)
Linear Noise Approximation (LNA)	0.4953	(0.4934, 0.4971)

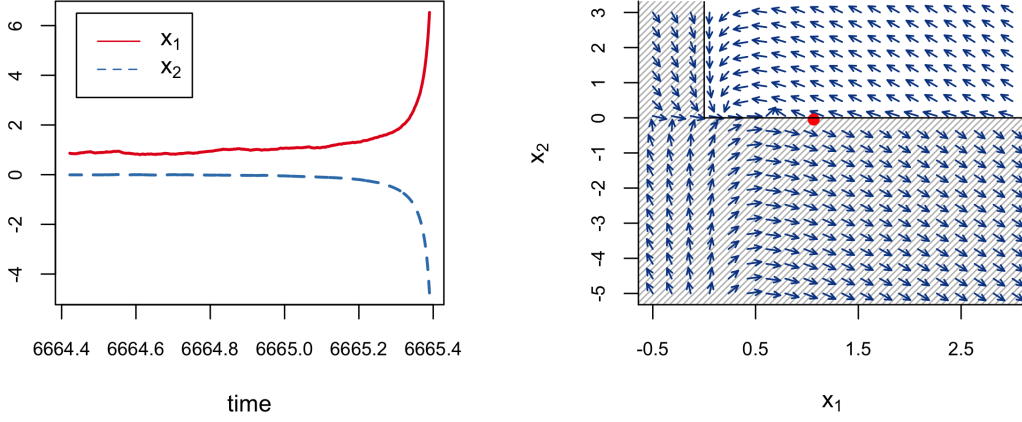


Figure 7: (Left) Real parts ( $x_1$  and  $x_2$ , representing concentration for species  $S_1$  and  $S_2$ , respectively) for a simulation of the complex Langevin approximation of the system given by (54) with parameters  $r = 100$ ,  $\alpha_1 = \beta_1 = 1$ ,  $\nu = 10$ ,  $\alpha_2 = 0.02$ , and  $\beta_2 = 5$ . (Right) Direction vector field for the drift (normalized to have unit length) of the complex Langevin approximation computed for the same simulation at time  $t = 6665$ , where the real parts of  $x_1$  and  $x_2$  are given by 1.0655 and  $-0.0483$ , respectively, (shown as a red dot) and their imaginary parts are given by  $-0.0227$  and  $0.0376$ , respectively. The vector field shown was computed for values in the real  $x_1$ - $x_2$  plane with the imaginary parts fixed to  $-0.0227$  and  $0.0376$  for  $x_1$  and  $x_2$ , respectively.

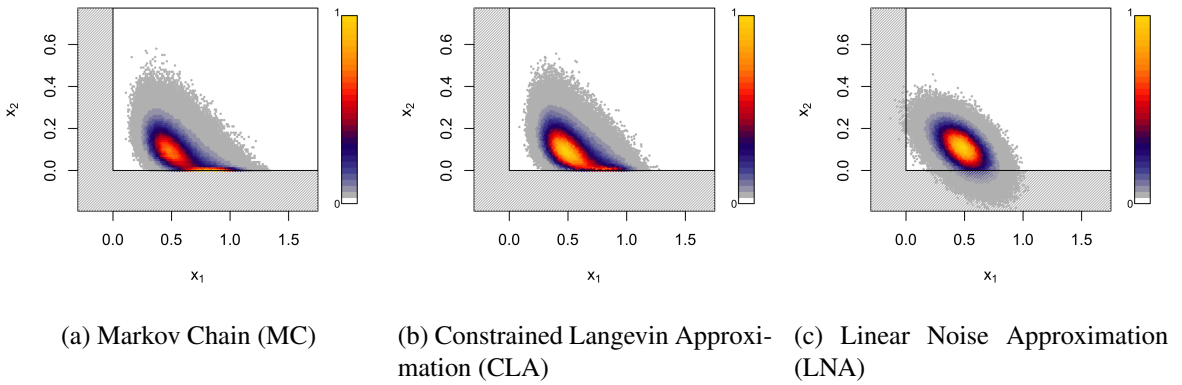


Figure 8: Scatter plot of the concentrations of  $S_1$  and  $S_2$ , given by  $x_1$  and  $x_2$ , respectively, generated from simulations of the MC, CLA and LNA for the system given by (54) with parameters  $r = 100$ ,  $\alpha_1 = \beta_1 = 1$ ,  $\nu = 10$ ,  $\alpha_2 = 0.02$ , and  $\beta_2 = 5$ . The complex Langevin approximation is not shown here since the approximation diverges during a long simulation (see Figure 7).

## 5 Summary and Discussion

It is attractive, both analytically and computationally, to approximate a continuous time, discrete state space Markov chain by a continuous time, continuous state diffusion process. From a modeling perspective this step involves replacing integer-valued molecule counts by real-valued concentration levels. It is intuitively clear that this modeling choice is likely to run into difficulties when one or more species has a small molecule count. This issue may manifest itself at a practical level by the solution path taking non-physical negative values. From a technical perspective, the diffusion process may not remain well-defined. Our aim in this work was to address this issue by introducing obliquely reflected diffusions as constrained Langevin approximations. The behavior of these diffusions matches that of solutions to the standard chemical Langevin equation in the interior of the positive orthant and introduces an appropriate minimal perturbation at the boundary. Our formal derivation of the constrained Langevin approximation was backed up by analytical and computational examples that illustrate the benefits of the approach. A complementary, more rigorous, derivation of this diffusion approach, which includes existence and uniqueness proofs, has been developed in [27].

A direction for further work that we are pursuing is the development of error estimates for the constrained Langevin approximation as an approximation to the underlying Markov chain, both at the transient and steady-state level. In another vein, the type of diffusion approximation proposed here is also likely to be of interest for researchers considering other continuous time Markov chains that live in the positive orthant, e.g., in population genetics and neuroscience. The authors would appreciate hearing from researchers interested in such models and approximations.

**Acknowledgements.** The genesis of this work was in informal discussions between DFA, DJH and RJW at a workshop on Multi-scale Stochastic Modeling of Cell Dynamics held at the Banff International Research Station in 2010. We are grateful to the organizers of that workshop for making this serendipitous connection possible. An extended abstract of the current paper is included in the Report of the Oberwolfach Workshop on Reaction Networks and Population Dynamics, June 18-24, 2017 [5]. Research of DFA was supported by NSF grant DMS-1318832 and Army Research Office grants W911NF-14-1-0401 and W911NF-18-1-0324. Research of DJH was supported by grant EP/M00158X/1 from the EPSRC/RCUK Digital Economy Programme and by grant EP/P020720/1 from the EPSRC. Research of RJW was supported in part by NSF grants DMS-1463657 and DMS-1712974. Research of SCL was supported by CAPES Process No. 23071.012226/2013-06 and by FAPEMIG Process No. APQ 00945/14.

## A Brief introduction to obliquely reflected diffusion processes

In this appendix, for the benefit of the reader, we give a very brief summary of some aspects of obliquely reflected diffusion processes as they pertain to the constrained Langevin approximation (CLA) described in this paper.

Let  $\mathcal{G}^o$  be a non-empty domain in  $\mathbb{R}^m$ ,  $\gamma : \partial\mathcal{G} \rightarrow \mathbb{R}^m$  be a unit length vector field defined on the boundary  $\partial\mathcal{G}$  of  $\mathcal{G}^o$ , and  $\mu : \mathcal{G} \rightarrow \mathbb{R}^m$  and  $\sigma : \mathcal{G} \rightarrow \mathbb{S}_+^m$  be continuous functions defined on the closure,  $\bar{\mathcal{G}}$ , of  $\mathcal{G}^o$ . Here  $\mathbb{S}_+^m$  denotes the set of  $m \times m$  positive semi-definite matrices. Informally, a reflected diffusion associated with the parameters  $(\mathcal{G}^o, \gamma, \mu, \sigma)$  is a continuous (strong) Markov process that behaves in the domain  $\mathcal{G}^o$  like a solution of the Langevin equation with (state-dependent) drift  $\mu$  and dispersion  $\sigma$ , and that is constrained to live in the closure  $\bar{\mathcal{G}}$  of  $\mathcal{G}^o$  by a control at the boundary which acts in the (state-dependent) direction of the vector field  $\gamma$ . This type of control is often referred to as a singular control because it only acts when the diffusion process is on the boundary, and typically the amount of time that the diffusion process spends on the boundary has zero Lebesgue measure (and so the control acts only at a singular set of



times).

One possible way<sup>9</sup> to try to define such a process precisely is to require it to be a continuous process  $\mathfrak{Z}$  taking values in  $\mathcal{G}$  that is a solution of the following Stochastic Differential Equation with Reflection (SDER):

$$\mathfrak{Z}(t) = \mathfrak{Z}(0) + \int_0^t \mu(\mathfrak{Z}(s)) ds + \int_0^t \sigma(\mathfrak{Z}(s)) dW(s) + \int_0^t \gamma(\mathfrak{Z}(s)) d\mathfrak{L}(s), \quad t \geq 0, \quad (55)$$

where  $W$  is a standard  $m$ -dimensional Brownian motion, the stochastic integral with respect to  $W$  is an Itô integral, and  $\mathfrak{L}$  is a continuous, non-decreasing, one-dimensional process that satisfies  $\mathfrak{L}(0) = 0$  and  $\mathfrak{L}$  can only increase when  $\mathfrak{Z}$  is on  $\partial\mathcal{G}$ , that is,  $\int_0^\infty 1_{\{\mathfrak{Z}(s) \notin \partial\mathcal{G}\}} d\mathfrak{L}(s) = 0$ . Here  $\mathfrak{L}(t)$  is the cumulative amount of control (or “pushing”) exerted at the boundary, in the direction of the vector field  $\gamma$ , up to time  $t$ . Note that with  $\mathfrak{Z}, \mathfrak{L}$  replaced by  $\tilde{Z}^r, \frac{1}{\sqrt{r}}\tilde{L}^r$ , and  $\sigma$  replaced by  $\frac{1}{\sqrt{r}}\sigma$ , (55) has the form of our CLA (33).

For historical reasons, a solution  $\mathfrak{Z}$  of (55) is called a reflected diffusion process, although the constraining action at the boundary is more like regulation or control. The origin of the term “reflection” lies in the fact that when  $m = 1$ ,  $\mathcal{G}^o = (0, \infty)$ ,  $\mu = 0$ ,  $\sigma = 1$ ,  $\gamma = 1$  and  $\mathfrak{Z}(0) = 0$ ,  $(\mathfrak{Z}, \mathfrak{L})$  is equivalent in distribution to  $(|B|, L)$  where  $B$  is a standard one-dimensional Brownian motion,  $|B|$  is its reflection about the origin, and  $\mathfrak{L}$  is the “local time” of  $|B|$  at the origin, which satisfies  $L(t) = \lim_{\epsilon \rightarrow 0} \frac{1}{2\epsilon} \int_0^t 1_{[0, \epsilon)}(|B|(s)) ds$  almost surely, and is a normalized measure of the amount of time that  $|B|$  spends near the origin. Indeed, by Tanaka’s formula [9],

$$|B(t)| = \int_0^t \text{sgn}(B(s)) dB(s) + L(t), \quad t \geq 0, \quad (56)$$

where  $\text{sgn}(x) = +1$  if  $x > 0$ ,  $= -1$  if  $x < 0$ , and  $= 0$  if  $x = 0$ ; and  $\{\int_0^t \text{sgn}(B(s)) dB(s), t \geq 0\}$  defines another standard one-dimensional Brownian motion. On setting  $W(t) = \int_0^t \text{sgn}(B(s)) dB(s)$  for  $t \geq 0$ , we see that  $(\mathfrak{Z}, \mathfrak{L}) = (|B|, L)$  is a solution of (55) when  $(\mathcal{G}^o, \mu, \sigma, \gamma) = ((0, \infty), 0, 1, 1)$ . For more details on this reflected Brownian motion case, see Chapters 7 and 8 of [9]. Although a mirror reflection construction of solutions of (55) does not generally hold for non-zero  $\mu$ , state-dependent  $\sigma$ , or  $\gamma$  and  $\mathcal{G}^o$  in higher dimensions, the term “reflected diffusion” has nevertheless been widely used in the literature for processes of the form (55). We now describe the results relevant to existence and uniqueness of solutions of (55) beyond the simple one-dimensional Brownian motion case just described.

Of course, in general, additional conditions need to be imposed on  $\mathcal{G}^o$ ,  $\gamma$ ,  $\mu$  and  $\sigma$  in order for (55) to be well posed. For our CLA,  $\mathcal{G}^o$  is naturally a polyhedral domain, and in all but one-dimension, or in situations that can be reduced to such, the boundary will be nonsmooth, although it will be piecewise smooth. Also, if  $\mu \neq 0$  on  $\partial\mathcal{G}$ , then  $\gamma = \mu/|\mu|$  can be extended to a smooth (in fact,  $C^\infty$ ) function in a neighborhood of  $\partial\mathcal{G}$ .

In [11], Dupuis and Ishii considered the problem of existence and uniqueness of solutions of equations like (55) when the boundary of  $\mathcal{G}$  is not smooth. The first of two cases that they treated is relevant to CLAs as it allows for a smooth, state-dependent vector field  $\gamma$  defined on a nonsmooth boundary. For that case, they assume that  $\mathcal{G}^o$  is a bounded domain,  $\gamma$  can be extended to a  $C^2$ , unit-length vector field on all of  $\mathbb{R}^m$ , and  $\mu$  and  $\sigma$  are uniformly Lipschitz continuous on  $\mathcal{G}$ . They formulate sufficient conditions for the existence and uniqueness of “strong”<sup>10</sup> solutions of (55). The critical condition (3.2) in their paper requires that, at each point on the boundary, the vector field  $\gamma$  points into  $\mathcal{G}^o$  in a suitably strong way. Unfortunately, due to topological constraints, such an inward pointing vector field cannot be globally extended to be smooth and of unit length on all  $\mathbb{R}^m$  (see [27] for a counterexample). However, as shown in Section 5 of [27], the existence and uniqueness result of [11] is in fact true with only local extendability of  $\gamma$ . In [27], Leite and

<sup>9</sup>An alternative approach is to try to characterize such processes in a distributional sense via submartingale problems, as first introduced by Stroock and Varadhan [35] for reflected diffusions in smooth domains and extended by various authors. See [21] for references on the two approaches and development of the relationship between them.

<sup>10</sup>A strong solution is required to be adapted to the filtration generated by  $W$  and the initial condition  $\mathfrak{Z}(0)$ .

Williams further show that this existence and uniqueness result can be extended to where  $\mathcal{G}$  is the unbounded positive orthant in  $\mathbb{R}^m$ , under the assumptions described in our paragraph containing (34). In particular, with the results of Dupuis and Ishii (as extended in [27]) for bounded domains and those in [27] for the orthant, existence and uniqueness of solutions of our CLA (33) for all of the examples considered in this paper, as well as many others, can be obtained. We refer the interested reader to [11, 21, 27] for more details on reflected diffusions, especially in nonsmooth domains.

## References

- [1] D. F. Anderson, G. Craciun, and T. G. Kurtz, *Product-form stationary distributions for deficiency zero chemical reaction networks*, Bulletin of Mathematical Biology **72** (2010), no. 8, 1947–1970.
- [2] D. F. Anderson and T. G. Kurtz, *Continuous time Markov chain models for chemical reaction networks*, Design and Analysis of Biomolecular Circuits: Engineering Approaches to Systems and Synthetic Biology (H. Koepl et al., ed.), Springer, 2011, pp. 3–42.
- [3] ———, *Stochastic Analysis of Biochemical Systems*, Springer, 2015.
- [4] A. Angius, G. Balbo, M. Beccuti, E. Bibbona, A. Horvath, and R. Sirovich, *Approximate analysis of biological systems by hybrid switching jump diffusion*, Theoretical Computer Science **587** (2015), 49–72.
- [5] E. Baake, T. Kurtz, and C. Wiuf, *Reaction Networks and Population Dynamics*, Oberwolfach Reports **14** (2017), 1747–1804.
- [6] S. Bhardwaj and R. J. Williams, *Diffusion approximation for a heavily loaded multi-user wireless communication system with cooperation*, Queueing Systems **62** (2009), no. 4, 345–382.
- [7] R. Bhatia, *Matrix Analysis*, Springer, 1997.
- [8] M. Bossy, E. Gobet, and D. Talay, *A symmetrized Euler scheme for an efficient approximation of reflected diffusions*, Journal of Applied Probability **41** (2004), no. 3, 877–889.
- [9] K. L. Chung and R. J. Williams, *An Introduction to Stochastic Integration (2nd edition)*, Birkhauser, Boston, 1990.
- [10] A. Duncan, R. Erban, and K. Zygalakis, *Hybrid framework for the simulation of stochastic chemical kinetics*, Journal of Computational Physics **326** (2016), 398–419.
- [11] P. Dupuis and H. Ishii, *SDEs with oblique reflection on nonsmooth domains*, The Annals of Probability **21** (1993), no. 1, 554–580, Correction 36(5):1992-1997, 2008.
- [12] S. N. Ethier and T. G. Kurtz, *Markov Processes: Characterization and Convergence*, 2nd ed., John Wiley & Sons, New York, 2005.
- [13] A. Ganguly, D. Altintan, and H. Koepl, *Jump-diffusion approximation of stochastic reaction dynamics: Error bounds and algorithms*, Multiscale Model. Simul. **13** (2014), 1390–1419.
- [14] M. A. Gibson and J. Bruck, *Efficient exact stochastic simulation of chemical systems with many species and many channels*, The Journal of Physical Chemistry A **104** (2000), no. 9, 1876–1889.
- [15] D. T. Gillespie, *A general method for numerically simulating the stochastic time evolution of coupled chemical reactions*, Journal of Computational Physics **22** (1976), 403–434.

- [16] ———, *Exact stochastic simulation of coupled chemical reactions*, The Journal of Physical Chemistry **81** (1977), no. 25, 2340–2361.
- [17] ———, *Markov Processes: An Introduction for Physical Scientists*, Academic Press, 1991.
- [18] ———, *The chemical Langevin equation*, Journal of Computational Physics **113** (2000), no. 1, 297–306.
- [19] ———, *The chemical Langevin and Fokker-Planck equations for the reversible isomerization reaction*, The Journal of Physical Chemistry A **106** (2002), no. 20, 5063–5071.
- [20] T. Jahnke and M. Kreim, *Error bound for piecewise deterministic processes modeling stochastic reaction systems*, Multiscale Model. Simul. **10** (2016), 1119–1147.
- [21] W. Kang and K. Ramanan, *On the submartingale problem for reflected diffusions in domains with piecewise smooth boundaries*, The Annals of Probability **45** (2017), no. 1, 404–468.
- [22] W. N. Kang and K. Ramanan, *Characterization of stationary distributions of reflected diffusions*, Annals of Applied Probability **24** (2014), 1329–1374.
- [23] I. Karatzas and S. E. Shreve, *Brownian Motion and Stochastic Calculus*, 2nd ed., Springer-Verlag, New York, 1991.
- [24] J. Kómlós, P. Major, and G. Tusnady, *An approximation of partial sums of independent random variables and the sample distribution function*, Zeitschrift für Wahrscheinlichkeitstheorie und Verwandte Gebiete **32** (1975), 111–131.
- [25] T. G. Kurtz, *Strong approximation theorems for density dependent Markov chains*, Stochastic Processes and their Applications **6** (1977/78), 223–240.
- [26] ———, *Approximation of Population Processes*, CBMS-NSF Regional Conference Series in Applied Mathematics: 36, SIAM, 1981.
- [27] S. C. Leite and R. J. Williams, *A constrained Langevin approximation for chemical reaction networks*, To appear in the Annals of Applied Probability (2018), 1–66.
- [28] T. Manninen, M.-L. Linne, and K. Ruohonen, *Developing Itô stochastic differential equation models for neuronal signal transduction pathways*, Computational Biology and Chemistry **30** (2006), no. 4, 280–291.
- [29] G. Minas and D. A. Rand, *Long-time analytic approximation of large stochastic oscillators: Simulation, analysis and inference*, PLoS Computational Biology **13** (2017), no. 7, 1–23.
- [30] R Core Team, *R: A Language and Environment for Statistical Computing*, R Foundation for Statistical Computing, Vienna, Austria, 2018.
- [31] M. I. Reiman and R. J. Williams, *A boundary property of semimartingale reflecting Brownian motions*, Probability Theory and Related Fields **77** (1988), no. 1, 87–97.
- [32] J. Schnakenberg, *Simple chemical reaction systems with limit cycle behaviour*, Journal of Theoretical Biology **81** (1979), no. 3, 389–400.
- [33] D. Schnoerr, G. Sanguinetti, and R. Grima, *The complex chemical Langevin equation*, The Journal of Chemical Physics **141** (2014), no. 2, 024103.

- [34] M. Scott and B. P. Ingalls, *Using the linear noise approximation to characterize molecular noise in reaction pathways*, Proceedings of the AIChE Conference on Foundations of Systems Biology in Engineering (FOSBE), Santa Barbara, California, 2005.
- [35] D. W. Stroock and S. R. S. Varadhan, *Diffusion processes with boundary conditions*, Communications on Pure and Applied Mathematics **24** (1971), no. 2, 147–225.
- [36] L. Szpruch and D. J. Higham, *Comparing hitting time behavior of Markov jump processes and their diffusion approximations*, Multiscale Modeling & Simulation **8** (2010), no. 2, 605–621.
- [37] H. Tanaka, *Stochastic differential equations with reflecting boundary condition in convex regions*, Hiroshima Mathematical Journal **9** (1979), 163–177.
- [38] K. Tomita, T. Ohta, and H. Tomita, *Irreversible circulation and orbital revolution hard mode instability in far-from-equilibrium situation*, Progress of Theoretical Physics **52** (1974), no. 6, 1744–1765.
- [39] N. G. van Kampen, *A power series expansion of the master equation*, Canadian Journal of Physics **39** (1961), 551–567.
- [40] ———, *Stochastic Processes in Physics and Chemistry*, 3rd ed., Elsevier, North-Holland Personal Library, 2007.
- [41] E. W. J. Wallace, L. R. Petzold, D. T. Gillespie, and K. R. Sanft, *Linear noise approximation is valid over limited times for any chemical system that is sufficiently large*, IET Systems Biology **6** (2012), no. 4, 102–115.
- [42] J. Wilkie and Y. M. Wong, *Positivity preserving chemical Langevin equations*, Chemical Physics **353** (2008), 132–138.
- [43] D. J. Wilkinson, *Stochastic Modelling for Systems Biology*, Chapman and Hall/CRC Press, 2006.